Journal Pre-proof

2-Styryl-4-aminoquinazoline derivatives as potent DNA-cleavage, p53-activation and *in vivo* effective anticancer agents

Xin-Wei Wei, Jing-Mei Yuan, Wan-Yun Huang, Nan-Ying Chen, Xiao-Juan Li, Cheng-Xue Pan, Dong-Liang Mo, Gui-Fa Su

PII: S0223-5234(19)31003-7

DOI: https://doi.org/10.1016/j.ejmech.2019.111851

Reference: EJMECH 111851

To appear in: *European Journal of Medicinal Chemistry*

Received Date: 7 August 2019

Revised Date: 3 November 2019

Accepted Date: 3 November 2019

Please cite this article as: X.-W. Wei, J.-M. Yuan, W.-Y. Huang, N.-Y. Chen, X.-J. Li, C.-X. Pan, D.-L. Mo, G.-F. Su, 2-Styryl-4-aminoquinazoline derivatives as potent DNA-cleavage, p53-activation and *in vivo* effective anticancer agents, *European Journal of Medicinal Chemistry* (2019), doi: https://doi.org/10.1016/j.ejmech.2019.111851.

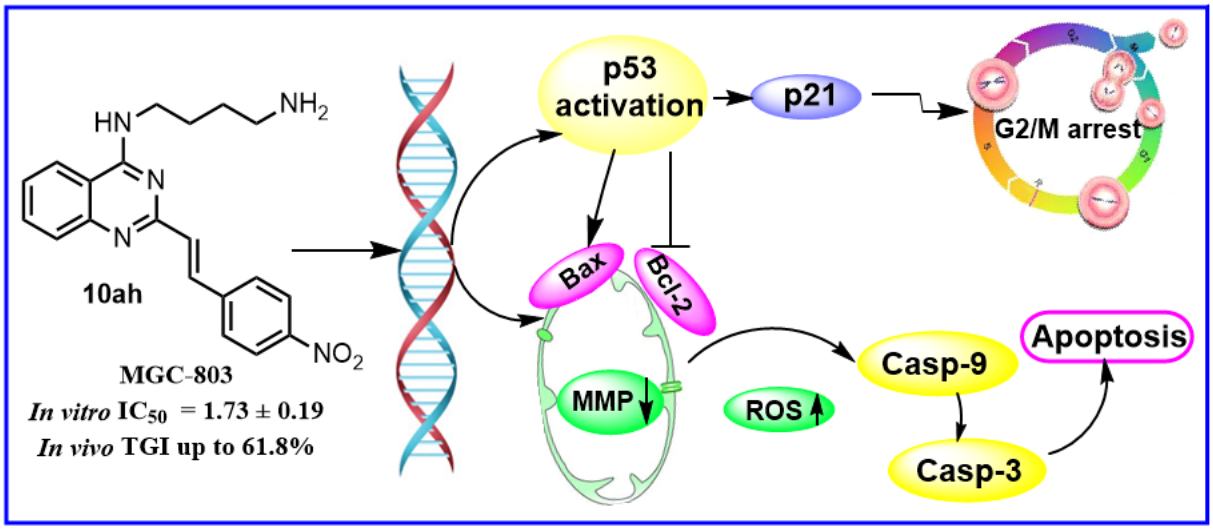

2-Styryl-4-aminoquinazoline derivatives as potent DNA-cleavage, p53-activation and *in vivo* effective anticancer agents

Xin-Wei Wei[a†], Jing-Mei Yuan[a†], Wan-Yun Huang[b], Nan-Ying Chen[a], Xiao-Juan Li[a], Cheng-Xue Pan[a]*, Dong-Liang Mo[a]*, Gui-Fa Su[a]*

[a]*State Key Laboratory for the Chemistry and Molecular Engineering of Medicinal Resources, School of Chemistry and Pharmaceutical Sciences, Guangxi Normal University, Guilin 541004, PR China*

[b]*Department of Pharmacology, Guilin Medical University, Guilin 541004, PR China*

[†] These authors contributed equally to this work.

* Corresponding Authors: Professors Cheng-Xue Pan, Dong-Liang Mo, and Gui-Fa Su

Tel. & Fax: +86-773-3696862, Email: chengxuepan@163.com (C.-X. Pan); moeastlight@gxnu.edu.cn (D.-L. Mo); gfysglgx@163.com (G.-F. Su)

ABSTRACT

Forty-eight analogues of CP-31398, an antitumor agent modulated the mutant *p53* gene were synthesized and their cytotoxicities against four cancer cell lines with different p-53 status including bladder cell T24 (w-p53), gastric cell MGC-803 (m-p53), prostate cell DU145 (m-p53), prostate cell PC-3 (null-p53), lung cell A549 (w-p53) and normal liver cell line HL-7702 (w-p53) were examined. (*E*)-2-(4-Nitrostyryl)-4-(3-dimethylaminopropyl)-aminoquinazoline (**10ah**) was identified as the most potent compound in anti-proliferation against MGC-803 cells, with IC_{50} lowed to 1.73 μM, far potency than that of CP-31398.

Molecular mechanism study revealed that **10ah** and CP-31398 differ greatly in mechanism to exert their antitumor properties. **10ah** could intercalate into DNA and resulted in significant DNA double-strand break. **10ah**-treatment in MGC-803 cells increased the expression of p53, phosphorylated p53 (p-p53), CDK4, p21 to cause cell cycle arrest at G2/M phase, significantly up-regulated the levels of pro-apoptosis proteins Bak, Bax, Bim while down-regulated the anti-apoptosis proteins Bcl-2, Bcl-xL and the levels of cyclin B1, fluctuated the intracellular reactive oxygen species (ROS), Ca^{2+} and mitochondrial membrane potential, activated Caspase-9 and Caspase-3 to induce apoptosis. **10ah** also displayed potent anticancer efficiency against MGC-803 xenograft tumors models, with tumor growth inhibition (TGI) up to 61.8% at 20 mg/kg without obvious toxicity.

Keywords: 2-Styryl-4-aminoquinazoline; CP-31398, DNA intercalator; Anticancer; Synthesis

1. Introduction

2-Styryl-4-aminoquinazoline or 2-styryl-4-chloroquinazoline derivatives exhibit diverse bioactivities such as antitumor [1-6], antibacterial [7-9], analgesic [10], anti-inflammatory [11], antiprotozoal [12] and antiviral activity [13]. The most famous compound was CP-31398, which had been reported to exert antitumor activity via restoring the active conformation of mutated p53 to rescue its tumor suppressor functions [2, 14-16], or targeting both the wild and mutant-type p53 and block the growth of rhabdomyosarcoma [17]. Some more recent study also indicated that CP-31398 is able to revers the epithelial mesenchymal transition via the downregulation of PAX2s [18], or to down-regulate the p53 negative regulator MDM2 in certain cancer [19]. Compound KIN-281 and KIN-236 were reported to show effects on inhibiting a wide range of tumor-related kinase proteins [1-4] (Fig. 1).

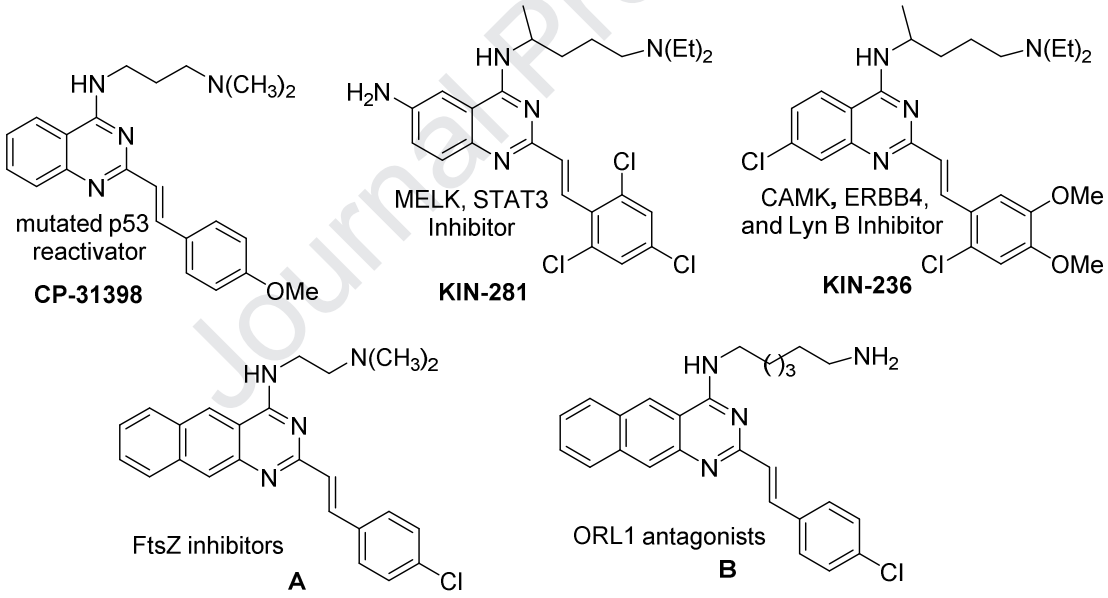

Fig. 1. Representative bioactive 2-styryl-4aminoquinazoline derivatives reported in literature

Besides anticancer activity, other 2-styryl-4-aminoquinazoline derivatives such as compound **A** was identified as promising anti-bacterial agent via inhibiting the cell division protein FtsZ [8-9], compound **B** as a highly selective opioid receptor like-1 (ORL1) antagonists [10] (Fig. 1).

Based on the summarization above, it can be seen that slight change on the substituents of 2-styryl-4-aminoquinazoline scaffold can results in great variety of

their bioactivity, which means that spent more efforts on the synthesis and bioactive evaluation of more novel 2-styryl-4-aminoquinazolines derivatives, might help to identify more novel candidates for drug development.

As our on going interest on the compounds that can regulate the p53 pathway [20-21], we decided to synthesize more novel analogues of CP-31398 and then explore their bioactivity in the aim of identifying new candidates for new antitumor drug development. Herein, we report the synthesis, *in vitro* and *in vivo* anticancer evaluation of a series of 2-styryl-4-aiminoquinazoline derivatives.

2. Results and discussion

2.1. Chemistry

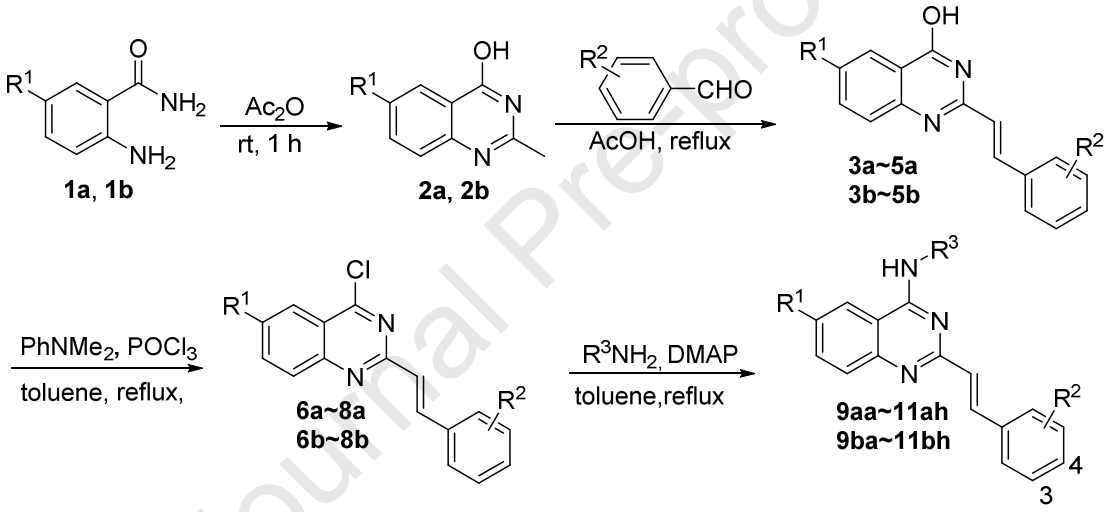

R^1: H (**a**), Cl (**b**); R^2: 3, 4-$(OCH_3)_2$ (**3, 6, 9**), 4-NO_2 (**4, 7, 10**), 3, 4-OCH_2O- (**5, 8, 11**);

R^3: $(CH_3)_2N(CH_2)_2$ (**a**), $(C_2H_5)_2N(CH_2)_2$ (**b**), $(i\text{-}Pr)_2N(CH_2)_2$ (**c**), 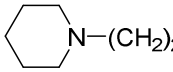

(**d**),

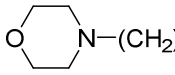

(**e**), $(CH_3)_2N(CH_2)_3$ (**f**), $(C_2H_5)_2N(CH_2)_3$ (**g**), $(CH_2)_4NH_2$ (**h**)

Scheme 1. Synthesis of 2-styryl-4-aiminoquinazoline derivatives **9-11**

The preparation of the target compounds were outlined in scheme 1. Stirring the mixture of 2-aminobenzamide derivatives **1** and excess anhydride at room temperature gave the compounds **2**, which were further condensed with aromatic aldehyde in acetic acid at 120 °C to provide the **3-5** in moderate yields.

Heating **3-5** with $POCl_3$ in the presence of *N*,*N*-dimethylaniline in toluene at 115 °C offered the intermediate **6-8**, respectively. In this step the presence of tertiary

amine as base was necessarily to smoothly finish the reaction, and we found that the *N*,*N*-dimethylaniline was more preferable than triethylamine or diisopropyl ethylamine. The intermediate **6-8** were very difficult to dissolve in any common solvents, so their structures could not be characterized by NMR. Finally, refluxing of **6-8** with amine derivatives in toluene in the presence of catalytic amount of DMAP furnished the targeted compounds **9-11** in moderate to high yields.

2.2. Biological activity

*2.2.1. Antiproliferative activity of compounds **9-11***

To obtain more information about the *in vitro* cytotoxic potency of the target 2-styryl-4-aminoquinazoline derivatives **9-11**, five human cancer cell lines from four different tissue, and in which also include the wild-type (w-p53), mutant-type (m-p53) and null-p53 three status of p53 gene were selected to evaluate the cytotoxicity of **9-11** via MTT assay. Epirubicin and CP-31398 were used as the positive control. The tested cell included the cancer cell lines T24 (from bladder, w-p53), MGC-803 (gastric cell, m-p53), DU145 (from prostate, m-p53), PC-3 (from prostate, null-p53), A549 (from lung, w-p53), the normal cell line HL-7702 (from liver, w-p53) and the IC_{50} values was summarized in table 1

Table 1 Structures and *in vitro* cytotoxicity of compounds **9**–**11**

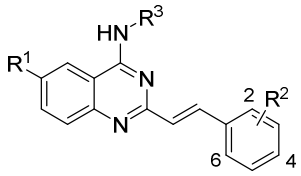

Comp.	R^1, R^2	R^3	IC_{50} (μM)[a] T24 w-*p53*	MGC-803 m-*p53*	DU145 m-*p53*	PC-3 null-*p53*	A549 w-*p53*	HL-7702 w-*p53*
9aa	H, 3,4-$(OCH_3)_2$	$(CH_3)_2N(CH_2)_2$	>100	>100	>100	>100	>100	>100
9ab	H, 3,4-$(OCH_3)_2$	$(C_2H_5)_2N(CH_2)_2$	30.20 ±2.98	>100	31.4 ±1.85	50.32 ±1.01	>100	>100
9ac	H, 3,4-$(OCH_3)_2$	(*i*-Pr)$_2$N$(CH_2)_2$	6.50 ±0.53	15.52 ±0.72	15.01 ±1.22	20.31 ±0.64	38.78 ±2.01	>100
9ad	H, 3,4-$(OCH_3)_2$	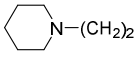	10.48 ±0.61	33.23 ±0.88	71.63 ±1.87	78.54 ±2.14	82.67 ±1.09	19.83 ±0.99
9ae	H, 3,4-$(OCH_3)_2$	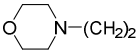	>100	>100	>100	>100	>100	>100
9af	H,	$(CH_3)_2N(CH_2)_3$	88.44	>100	>100	>100	>100	>100

	3,4-$(OCH_3)_2$		±1.96					
9ag	H, 3,4-$(OCH_3)_2$	$(C_2H_5)_2N(CH_2)_3$	>100	>100	>100	>100	>100	>100
9ah	H, 3,4-$(OCH_3)_2$	$(CH_2)_4NH_2$	30.89 ±0.49	70.46 ±0.53	>100	>100	>100	>100
10aa	H, *p*-NO_2	$(CH_3)_2N(CH_2)_2$	8.95 ±0.84	14.37 ±1.07	15.74 ±0.94	51.09 ±1.38	33.94 ±1.44	17.96 ±1.39
10ab	H, *p*-NO_2	$(C_2H_5)_2N(CH_2)_2$	>100	>100	>100	>100	>100	44.46 ±1.25
10ac	H, *p*-NO_2	$(i\text{-Pr})_2N(CH_2)_2$	14.23 ±0.47	29.05 ±1.88	>100	>100	>100	8.96 ±0.49
10ad	H, *p*-NO_2	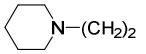	36.16 ±1.33	27.57 ±1.18	>100	25.61 ±0.97	28.23 ±1.41	>100
10ae	H, *p*-NO_2	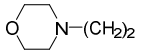	>100	>100	>100	>100	>100	>100
10af	H, *p*-NO_2	$(CH_3)_2N(CH_2)_3$	9.16 ±0.83	15.73 ±1.47	24.40 ±1.04	>100	59.54 ±1.90	21.40 ±0.56
10ag	H, *p*-NO_2	$(C_2H_5)_2N(CH_2)_3$	5.42 ±0.23	8.25 ±0.36	12.30 ±1.30	15.43 ±0.76	>100	5.30 ±1.48
10ah	H, *p*-NO_2	$(CH_2)_4NH_2$	**1.79 ±0.16**	**1.73 ±0.19**	**4.15 ±0.32**	**4.53 ±0.28**	**5.48 ±0.98**	**7.46 ±0.31**
11aa	H, 3,4-OCH_2O-	$(CH_3)_2N(CH_2)_2$	66.44 ±1.78	>100	>100	>100	>100	57.84 ±1.01
11ab	H, 3,4-OCH_2O-	$(C_2H_5)_2N(CH_2)_2$	8.68 ±0.47	9.88 ±0.19	16.34 ±0.99	33.86 ±1.96	46.90 ±2.17	20.71 ±1.43
11ac	H, 3,4-OCH_2O-	$(i\text{-Pr})_2N(CH_2)_2$	17.50 ±1.46	11.32 ±0.84	>100	>100	>100	21.24 ±1.56
11ad	H, 3,4-OCH_2O-	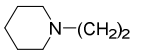	6.38 ±0.76	10.70 ±0.56	8.53 ±0.23	12.16 ±0.46	39.64 ±1.01	9.91 ±0.21
11ae	H, 3,4-OCH_2O-	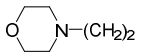	>100	>100	>100	>100	>100	>100
11af	H, 3,4-OCH_2O-	$(CH_3)_2N(CH_2)_3$	8.81 ±0.99	13.95 ±1.42	25.40 ±1.89	>100	>100	14.49 ±2.21
11ag	H, 3,4-OCH_2O-	$(C_2H_5)_2N(CH_2)_3$	>100	>100	>100	>100	>100	>100
11ah	H, 3,4-OCH_2O-	$(CH_2)_4NH_2$	41.18 ±0.93	24.58 ±0.49	>100	>100	>100	>100
9ba	Cl, 3,4-$(OCH_3)_2$	$(CH_3)_2N(CH_2)_2$	12.10 ±0.88	11.84 ±0.79	17.86 ±1.35	23.55 ±1.49	21.34 ±1.12	80.47 ±2.34
9bb	Cl, 3,4-$(OCH_3)_2$	$(C_2H_5)_2N(CH_2)_2$	12.17 ±0.77	16.75 ±0.38	>100	>100	>100	91.20 ±0.21
9bc	Cl, 3,4-$(OCH_3)_2$	$(i\text{-Pr})_2N(CH_2)_2$	14.85 ±0.43	15.56 ±0.75	>100	>100	>100	>100
9bd	Cl, 3,4-$(OCH_3)_2$	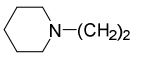	7.64 ±0.22	13.51 ±0.99	17.24 ±1.07	21.17 ±2.11	>100	13.86 ±0.39
9be	Cl, 3,4-$(OCH_3)_2$	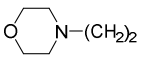	91.80 ±1.65	>100	>100	>100	>100	>100
9bf	Cl, 3,4-$(OCH_3)_2$	$(CH_3)_2N(CH_2)_3$	>100	>100	>100	>100	>100	>100
9bg	Cl, 3,4-$(OCH_3)_2$	$(C_2H_5)_2N(CH_2)_3$	**3.51 ±0.26**	**8.42 ±0.76**	**5.35 ±0.39**	**6.25 ±0.84**	**>100**	**5.17 ±0.73**
9bh	Cl, 3,4-$(OCH_3)_2$	$(CH_2)_4NH_2$	7.82 ±0.32	14.14 ±0.72	19.99 ±1.45	>100	50.50 ±4.45	>100
10ba	Cl, *p*-NO_2	$(CH_3)_2N(CH_2)_2$	**6.97 ±0.24**	**4.68 ±0.17**	**6.76 ±1.20**	**8.02 ±0.78**	**>100**	**71.34 ±1.49**
10bb	Cl, *p*-NO_2	$(C_2H_5)_2N(CH_2)_2$	11.04 ±0.77	7.12 ±0.34	12.41 ±1.64	>100	>100	>100
10bc	Cl, *p*-NO_2	$(i\text{-Pr})_2N(CH_2)_2$	56.64 ±1.57	17.27 ±1.43	>100	>100	>100	>100
10bd	Cl, *p*-NO_2	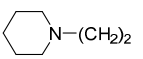	34.34 ±0.79	19.97 ±0.47	>100	>100	41.08 ±1.47	>100
10be	Cl, *p*-NO_2	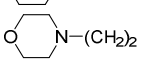	>100	>100	>100	>100	>100	>100
10bf	Cl, *p*-NO_2	$(CH_3)_2N(CH_2)_3$	**7.42 ±0.49**	**6.67 ±0.39**	**8.49 ±0.54**	**5.32 ±0.56**	**15.83 ±0.76**	**>100**
10bg	Cl, *p*-NO_2	$(C_2H_5)_2N(CH_2)_3$	**7.12 ±0.22**	**7.37 ±0.24**	**8.12 ±0.37**	**6.89 ±0.33**	**76.43 ±3.33**	**14.97 ±0.56**

10bh	Cl, *p*-NO_2	$(CH_2)_4NH_2$	5.62 ±0.55	9.16 ±0.67	>100	>100	10.03 ±1.67	>100
11ba	Cl, 3,4-OCH_2O-	$(CH_3)_2N(CH_2)_2$	9.61 ±0.94	9.46 ±0.78	>100	>100	>100	>100
11bb	Cl, 3,4-OCH_2O-	$(C_2H_5)_2N(CH_2)_2$	8.17 ±0.88	11.12 ±0.27	7.56 ±0.47	14.21 ±1.56	>100	15.91 ±2.37
11bc	Cl, 3,4-OCH_2O-	$(C_2H_5)_2N(CH_2)_2$	**7.46 ±0.82**	**8.57 ±0.48**	**8.78 ±0.57**	**10.57 ±0.68**	**>100**	**>100**
11bd	Cl, 3,4-OCH_2O-	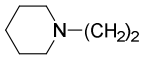	9.22 ±0.89	14.66 ±1.01	>100	>100	>100	>100
11be	Cl, 3,4-OCH_2O-	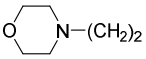	38.32 ±3.89	>100	>100	>100	>100	>100
11bf	Cl, 3,4-OCH_2O-	$(CH_3)_2N(CH_2)_3$	8.12 ±0.67	17.23 ±2.42	>100	>100	>100	>100
11bg	Cl, 3,4-OCH_2O-	$(C_2H_5)_2N(CH_2)_3$	9.74 ±0.37	12.94 ±1.20	>100	>100	>100	>100
11bh	Cl, 3,4-OCH_2O-	$(CH_2)_4NH_2$	5.65 ±0.24	10.31 ±0.39	50.29 ±1.20	>100	9.82 ±1.08	>100
C[b]			20.34 ±2.07	18.27 ±1.02	15.34 ±2.03	16.34 ±1.43	24.78 ±2.07	25.34 ±0.49
D[c]			1.12 ±0.33	1.20 ±0.31	2.01 ±0.47	2.31 ±0.51	0.82 ±0.17	2.10 ±0.51

[a] Results were expressed as means ± SD (standard deviation) of four independent experiments.

[b] **C**: CP-31398; [c] **D**: Epirubicin

As shown in table 1, most target compounds displayed moderate to potent inhibitory activities against the tested cancer cell lines. Compounds **10ah**, **9bg**, **10ba**, **10bf**, **10bg** and **11bc** exhibited especially potent cytotoxicity and **10ah** display exceptional efficacy against MGC-803 and T24 cancer cell lines, with IC_{50} values low to 1.73 and 1.79 μM, respectively, almost 8 and 11 folds potency than that of its analogue CP-31398 and close to that of the clinical antitumor drug Epirubicin.

The data in table 1 revealed that the series compounds display no much selectivity to the different p53 status of the cancer cell, indicating they can exert their anti-proliferation via a p53 independent manner. In 2015 and most recently, some p53 independent antitumor styrylquinoline derivatives were also reported by Musiol and Mrozek-Wilczewicz [22-23], which suggested that these styrylquinazoline derivatives, though different in structure to the styrylquinoline derivatives reported by Musiol and Mrozek-Wilczewicz, might share some common mechanism of action. Since mutations in the p53 gene are very common in cancers and are closely related to drug resistance and poor prognosis, compounds displaying anti-proliferation in a p53 independent manner are often considered to be a promising class of compounds that deserve further exploration[23]. In addition, the series compounds demonstrate somewhat selectivity to certain tissue of cancer cell. In general, the anti-proliferation against the T24 and MGC-803 cell lines are more potent than that against the other

three tested cell lines DU145, PC-3 and A549.

The results in table 1 indicated that the side chains at the 2-styryl-4-aminoquinazoline scaffold, the substituent on the phenyl ring of quinazoline motifs or the styryl all played very important roles in the anti-proliferation, but the substituents on the three position mentioned above seem significantly influence each other, which means that a seemingly favorable substituent at certain position, might probably mismatch with another favorable substituent at the other position. These complicated results of structure-activity relationship (SAR), might attribute to the fact that this 2-styryl-4-aminoquinazoline scaffold, might usually act as many kinase inhibitors, and a very subtle change in structure of the compounds would results in the mismatch with the structural domain of the certain kinase [2].

The data in table 1 also indicated that R^1 as Cl (**b** series) seemed more favorable than H (**a** series), and R^2 as 4-NO_2 (**10** series) more desirable than 3,4-$(OCH_3)_2$ (**9** series) or 3,4-(OCH_2CH_2O)- (**11** series) for the cytotoxic activities of the targeted compounds in general. As far as the effects of R^3 on the cytotoxicity was concerned, when R^3 is a primary amine (series **xxh**), a dialkylamine (series **xxa-c** and **xxf-g**) or a piperidinyl (series **9~11xe**), the cytotoxicity of the compounds and the kinds of R^3 seems no much obvious regularities and the only obvious SAR of R^3 able to summarize in table 1 was that compounds with a morpholinyl (series **9-11xe**) as R^3 almost display no any anti-proliferation activity. The complicated SAR results of this series 2-styryl-4-aminoquinazoline, suggested that to identify more potent antitumor drug candidates based on the 2-styryl-4-aminoquinazoline scaffold, more attention should be paid to the optimal matching of 2-styryl-4-aminoquinazoline matrix substituents at different positions.

Since compound **10ah** displayed the highest cytotoxicity against the tested tumor cells, especially to the MGC-803 and T24 cell lines, it was used as a representative compound to carry out the mechanism studies in MGC-803 cell.

*2.2.2. **10ah** intercalate into DNA and significantly induce DNA double-strand break*

DNA is believed to be one of the primary targets of the antitumor drug [24-27]. As many studies reported in literature mainly focused on how the 2-styryl-4-amino-quinazoline derivatives affecting and regulating the certain protein kinases [1-4], what

most interest us was whether **10ah** probably exerted its antitumor activity via target the DNA and to trigger the cascade reaction of antitumor-related pathway in tumor cells to induce apoptosis [28].

UV–Vis and fluorescence spectrophotometry were firstly used to investigate the interaction of **10ah** with ct-DNA. The UV–Vis spectra of **10ah** in the absence (dashed line) and presence of ct-DNA were shown in Fig. 2A. As the Fig. 2A indicated, **10ah** exhibit characteristic absorption peak at *ca*. 320~335 nm. With the addition of DNA, a corresponding decrease in the absorption intensity was observed, suggesting the **10ah** could bind to the DNA and result in a hypochromicity.

To confirm the interaction mode of **10ah** with DNA, competitive binding assay was further performed using the classic DNA intercalator ethidium bromide (EB) as a probe. As shown in Fig. 2B, the addition of **10ah** (the ratio of [**10ah**]/[DNA]/[EB] increasing from 0.5: 10: 1 to 5: 10: 1) could obviously result in the quenching of ct-DNA–EB fluorescence intensity. The result indicated that **10ah** could compete with EB and replace it to intercalate into ct-DNA [29] and the quenching constant Kq, according to the Stern-Volmer quenching equation, was calculated to be 1.08×10^4.

To determine whether **10ah** can intercalate into intact DNA, agarose gel electrophoresis assay was further used to investigate the interaction of **10ah** with pBR332 plasmid DNA, EB, a well-known of DNA intercalator able to directly intercalate into intact DNA, was used as the positive control. As indicated in Fig. 2C, a noticeable retardation of DNA movement was observed when the concentration of **10ah** was up to 100 μM, suggesting that **10ah** can directly intercalate into the intact DNA [29].

The level of γH2AX, a biomarker of DNA cleavage, was also measured by Western blotting assay in **10ah**-treated MGC-803 cells. As depicted in Fig. 2D, significantly increase in the level of γH2AX in **10ah**-treated MGC-803 cells was observed at 2.5 μM of **10ah**, indicating that **10ah** not only able to intercalate into DNA but induce substantial DNA double-strand break in MGC-803 cells. By comparing the performance of CP-31398 with that of compound **10ah** in Fig. 2C and D, suggesting that even very similarly in structure, **10ah** and CP-31398 might exert their antitumor properties via a completely different manner.

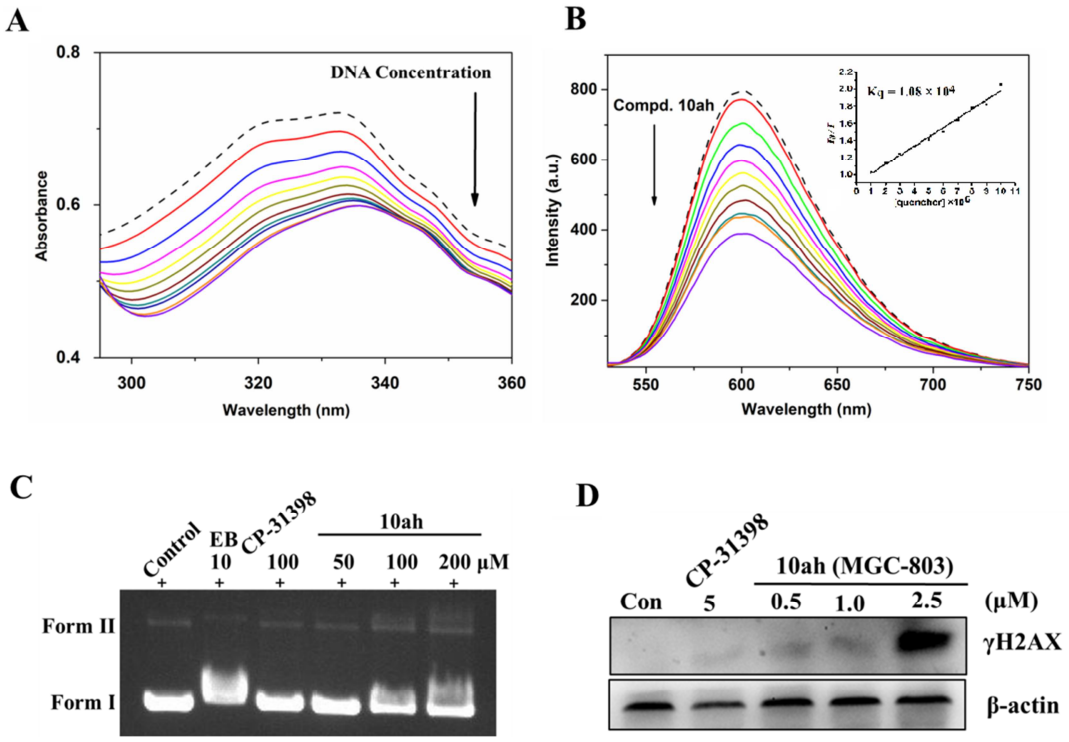

Fig. 2. DNA-binding properties of **10ah**. (A) UV/Vis spectra of compound **10ah** (20 μM) in Tris-HCl buffer with increasing amounts of ct-DNA ([ct-DNA]/[**10ah**] = 0~1.0) at 25 ℃. (B) Fluorescence emission spectra of EB bound with ct-DNA in the absence (dashed line) and presence of compound **10ah** as competitive agent with increasing [**10ah**]/[EB] ratios of 0.5: 1 to 5: 1. Inset: Plot of I_0/I versus [**10ah**] the quenching constant (Kq) of **10ah** towards ct-DNA-EB solution. (C) Gel electrophoresis of pBR322 DNA after being incubated with **10ah** at the concentrations of 50−200 μM for 3 h in Tris-HCl bu□er. 1% DMSO + pBR322 DNA in lane 1 as negative control, EB + pBR322 DNA in lane 2 as positive control, Lane 3 is the mixture of pBR322 DNA and 100 μM CP-31398. Other lanes are the mixture of pBR322 DNA and **10ah** (50, 100, 200 μM), respectively. (D) Immunoblotting analysis of γH2AX in CP-31398 and **10ah**-treated MGC-803 cells. Whole cell extracts were prepared and analyzed by Western blot. The data are representative of three independent experiments. *P < 0.05, **P < 0.01, ***P < 0.001 vs the negative control.

*2.2.3. **10ah** activate the p53 and induces cell cycle arrest in MGC-803 cells*

Since damage in DNA might usually result in the activation of p53 [30] to result

in cell cycle arrest, **10ah** and CP-31398 appear differently in interaction with DNA, the different effects of **10ah** and CP-31398 in the regulation of some key proteins in p53 signal pathway and cell cycle were firstly investigated. As shown in Fig. 3A-B, **10ah** substantially up-regulated the p53 and p-p53 (s15) levels in MGC-803 cells at lowed concentration while slightly enhanced the expression of its negative regulator MDM2 in p53 signal pathway. The level of some key cyclin, cyclin dependent kinases (CDK) or CDK inhibitor such as cyclin B1, CDK4 and p21 that are closely-related to the development in tumor in cell were also regulated by **10ah**. The cyclin B1 was significantly down-regulated and the expression of CDK4 and p21 were increased.

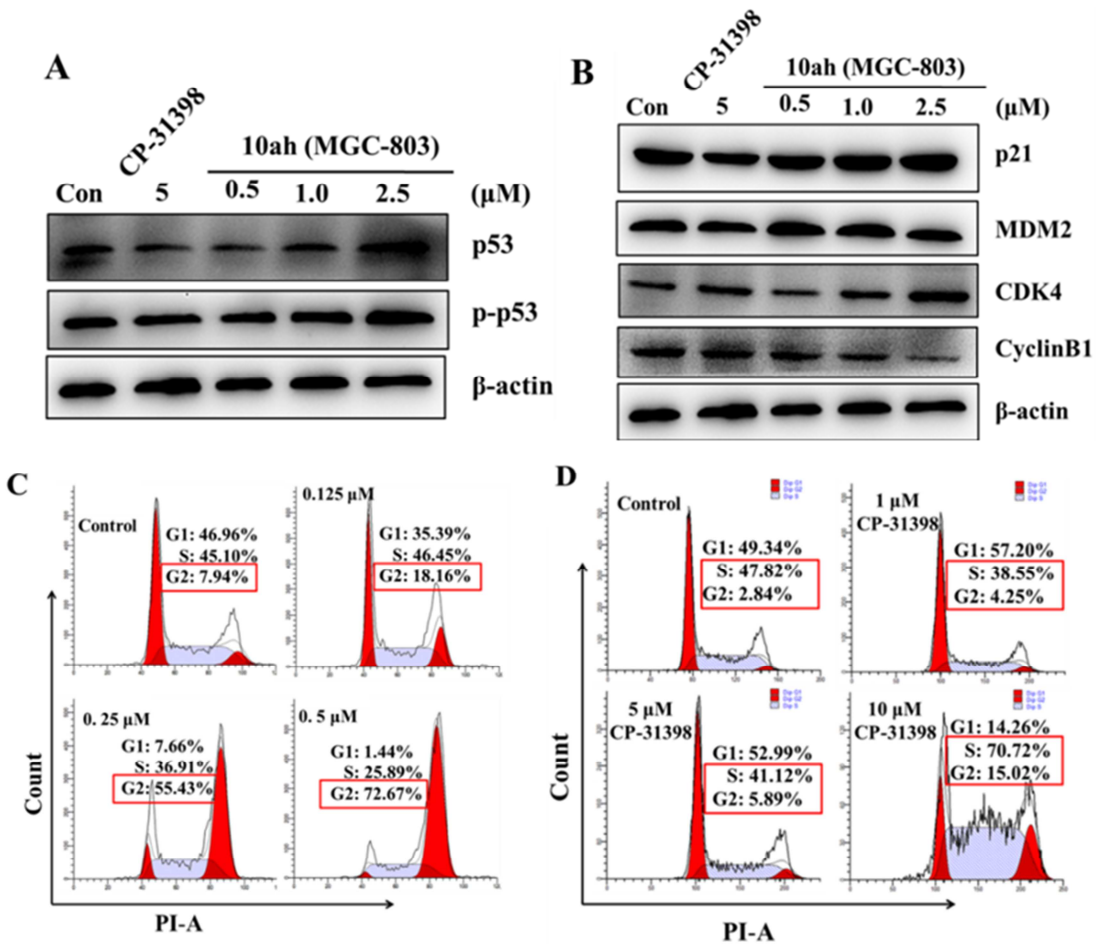

Fig. 3. (A) The expression levels of p53, p-p53 after treating of **10ah**. (B) The expression levels of p21, MDM2, CDK4 and Cyclin B1 after treating of **10ah**. CP-31398 was used as a positive control. *β*-actin was used as the loading control. (C) Compound **10ah** induced cell-cycle arrest in MGC-803 cells. (D) Cell cycle analysis of MGC-803 cells treated with various concentrations of CP-31398 for 48 h by flow cytometry. The data are representative of three independent experiments. *P < 0.05, **P < 0.01, ***P < 0.001 *vs* the negative control.

To further determine whether **10ah** inhibits the proliferation of MGC-803 cells through cell cycle arrest, flow cytometry was used to examine the cell cycle distribution of **10ah**-treated MGC-803 cells. As shown in Fig. 3C, with the increase of concentrations of **10ah**, the percentage of MGC-803 cells at G2/M phase was dramatically increased from 7.94% (Control group) to 18.16% (0.125 μM), 55.43% (0.25 μM) and 72.67% (0.5 μM) after **10ah**-treatment, indicating that **10ah**-treatment would result in remarked G2/M phase arrest in a dose–dependent manner.

In comparation with the results of CP-31398 treatment in MGC-803 cells, the expression of p53, p-p53, MDM2, cyclin B1 and p21 seems not to be obviously affected by CP-31398 at a concentration of 5.0 μM, only a slight increasing in CDK4 and the cell cycle is arrest in S and G2/M phase (Fig. 3D), suggested that the mechanism of **10ah** to exert it anticancer quite differ from that of CP-31398. As the report [12], PLC/PRL/5 cells (from liver, m-p53) treated by CP-31398 in a dose of 10 μg/mL (27.6 μM) would result in significantly up-regulating in the MDM2 and p21, while down-regulating in the cyclin B1 and inducing a G1 arrest, indicating that different cell treated by CP-31398 might have different performance in their p53 pathway and distribution in cell cycle.

*2.2.4. **10ah** affect the intracellular ROS, Ca^{2+} and MMP*

The balance of intracellular reactive oxygen species (ROS) [31] and Ca^{2+} [32] are very meaningful for the live and the normal physical activity of cells, an abnormal fluctuation of them in cell usually the indicator of apoptosis. To determine whether **10ah**-treatment MGC-803 cells would induce the production of ROS and fluctuation of Ca^{2+}, MGC-803 cells were treated with **10ah** and stained with 2′,7′-dichloro-dihydrofluorescein diacetate (DCFH-DA, fluorescent indicators for ROS) or Fluo-3 AM (fluorescent indicators for Ca^{2+}) at different doses for 24 h and the fluorescence intensities were measured.

As depicted in Fig. 4A, the fluorescence intensities indicating the amount of ROS were significantly increased, especially when the dose of **10ah** changed from 0 to 0.5 μM. While in Fig. 4B, the fluorescence intensities which indicated the level of

intracellular Ca^{2+} also increased steadily, suggesting that **10ah**-treament in MGC-803 cells would result in the increase of intracellular ROS and Ca^{2+} levels which may be responsible for apoptosis induction by **10ah**.

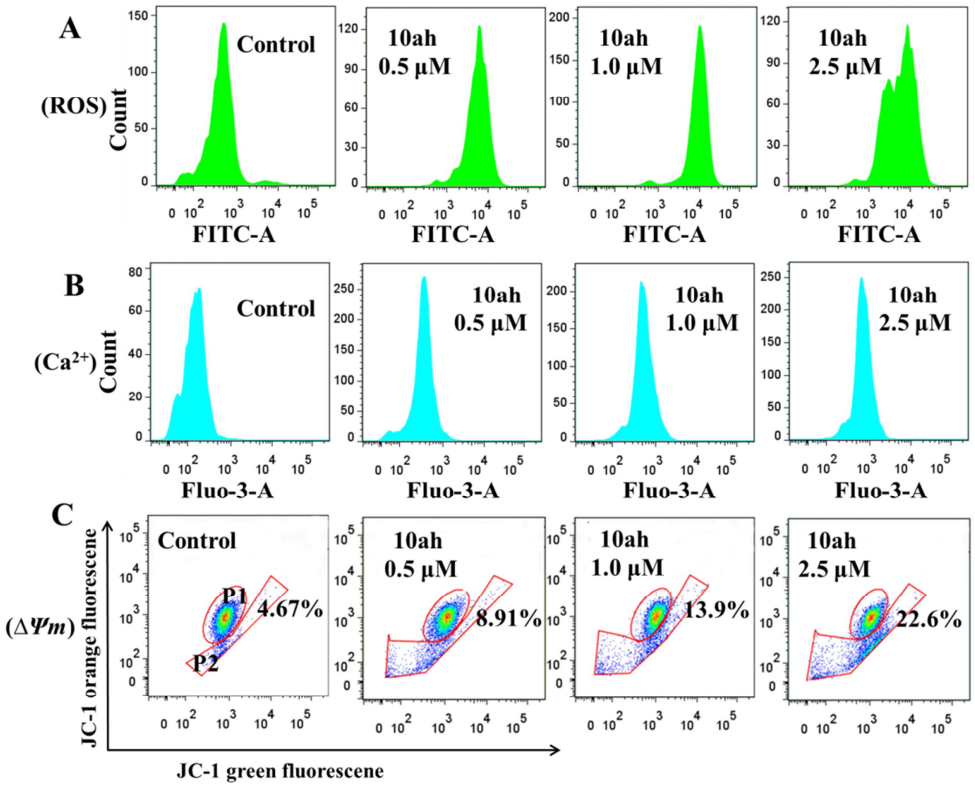

Fig. 4. (A) The generation of ROS after treatment with **10ah** for 24 h. (B) Effects of compound **10ah** on the intracellular Ca^{2+} level in MGC-803 cells. (C) The collapses of mitochondrial membrane potential treatment with compound **10ah** for 24 h. The data are representative of three independent experiments. *P < 0.05, **P < 0.01, ***P < 0.001 *vs* the negative control.

Mitochondrial membrane potential (MMP) is a critical parameter for understanding mitochondrial function [33] and the loss of MMP usually indicate the mitochondrial dysfunction associated with intrinsic mitochondrial apoptosis pathway [34]. To further get the information related to the pathway that mediated the cell apoptosis induced by **10ah**, the change of MMP of **10ah**-treated MGC-803 cells was measured by the fluorescent probe JC-1 (5,5',6,6'-tetrachloro-1,1',3,3'-tetraethyl-benzimidazolylcarbocyanine). As shown in Fig. 4C, in control group, weak green fluorescence (p2 region) which indicated a high $\Delta\Psi m$ was observed. While in **10ah**-treated cells the green fluorescence obviously increased in a dose-dependent manner, indicating the loss in MMP after **10ah** treatment in MGC-803 cells.

2.2.5. ***10ah*** *regulate the apoptosis related proteins to induce intrinsic apoptosis*

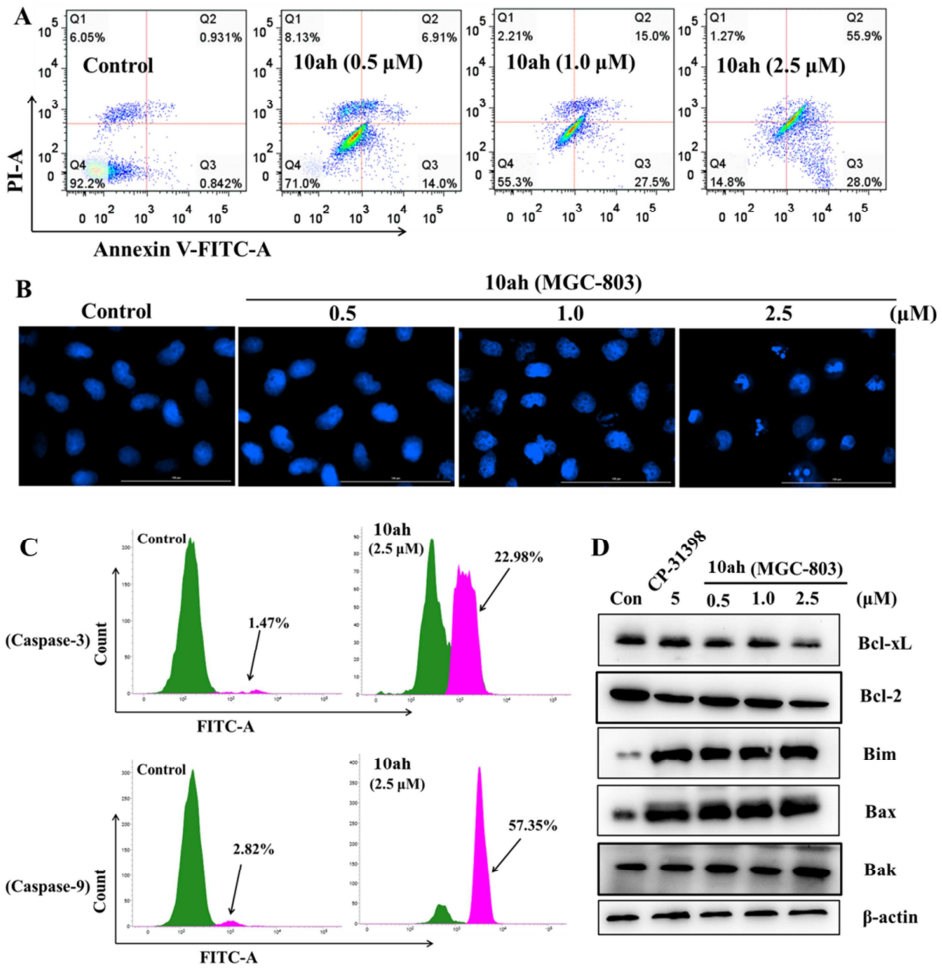

Fig. 5. 10ah induces cell apoptosis. (A) Apoptosis was detected by Annexin V-FITC/PI staining after cells treated with the indicated concentration of **10ah** for 24 h. (B) Morphology detection with Hoechst 33258 staining. (C) The activation of Caspase-3/9 by compound **10ah** in MGC-803 cells after treatment with 2.5 μM for 24 h. (D) Immunoblotting analysis of proteins related to the mitochondria-mediated intrinsic apoptotic pathway mediated by **10ah** and CP-31398. The data are representative of three independent experiments. *P < 0.05, **P < 0.01, ***P < 0.001 *vs* the negative control.

Apoptosis-inducing is still the basic way of the majority of clinical chemotherapeutic agent to exert their antitumor. To determine whether cell cycle arrest in MGC-803 cells result in apoptosis, Annexin V–FITC/PI staining and cell morphology analysis assay were used to evaluate the apoptosis-inducing effect. As

shown in Fig. 5A, with the increasing of **10ah** from 0 μM, 0. 5 μM, 1.0 μM to 2.5 μM, the percentages of the apoptotic cells increase dramatically from 1.7%, 20.9%, 42.5% to 83.9%, suggested that **10ah** could strongly induce apoptosis in MGC-803 cells. The result of cell morphology analysis via Hoechst 33258 staining depicted in Fig. 5B, also clearly indicated that **10ah**-treament result in cell shrinkage, nuclear fragmentation, chromatin condensation while non-treated cells displayed dispersal uniform fluorescence.

To gain more information about the pathway by which **10ah** mediated the apoptosis, the proportion of Caspase-3/9 activated cells after treatment with **10ah** was examined. As shown in Fig. 5C, the activation of Caspase-3 and Caspase-9 induced by **10ah** was clearly observed, as the proportion of Caspase-3 activated cells increased from 1.47% to 22.98% and the Caspase-9 activated cells from 2.82% to 57.35% when treating by 2.5 μM of **10ah**. These results indicated that **10ah** induced apoptosis via a caspase-dependent pathway in MGC-803 cells.

To gain further insight into the different mechanisms of tumor suppression activity of **10ah** and CP-31398 and which death effectors were the dynamic participants in the apoptosis signaling after **10ah** or CP-31398 treatment, first the levels of Bcl-2 family proteins in MGC-803 cells were measured after treated by **10ah** or CP-31398. As shown in Fig. 5D, the expression levels of pro-apoptotic proteins Bim and Bax were significantly up–regulated while the levels of anti-apoptotic proteins Bcl-2 were down–regulated both in the **10ah** or CP-31398 treatment cells, merely in CP-31398 treatment cells it needed more high concentration of drug, quite similar to the results in PLC/PRF/5 cell treated with CP-31398 report in literature [12]. The most different performance between the **10ah** and CP-31398 treatment cells could be observed in their levels of Bak and Bcl-xL, which were changed obviously in **10ah** treatment cells while almost unchanged in CP-31398 treatment.

*2.2.5. **10ah** shows potential anticancer potency in vivo*

The anticancer efficiency of **10ah** *in vivo* was examined in MGC-803 xenograft tumors. As shown in Fig. 6A-C, The MGC-803 xenograft tumor-bearing nude mice treated by **10ah** (10 or 20 mg/kg/2 days) displayed significant tumor growth inhibition. The *in vivo* tumor growth inhibition (TGI) of **10ah** and clinical drug Epirubicin were

35.9% (**10ah**, 10 mg/kg/2 days), 61.8% (**10ah**, 20 mg/kg/2 days), and 67.2% (Epirubicin, 10 mg/kg/2 days), respectively. By compared with the dose of CP-31398 (0.5 mg/mouse, about 30 mg/kg) treated in PLC/PRL/5 xenograft tumors to reach about 60% TGI [12], **10ah** need less dose than CP-31398 to obtain satisfaction treatment result, confirming the promising anticancer efficiency of **10ah** *in vivo*. The potential toxicity of **10ah** was also investigated by monitoring the weight loss of all tested nude mice. As depicted in Fig. 6D, no obvious changes in body weight were found in control group and treatment group during the treatment, indicating the low toxicity of **10ah** at the therapeutic dosage.

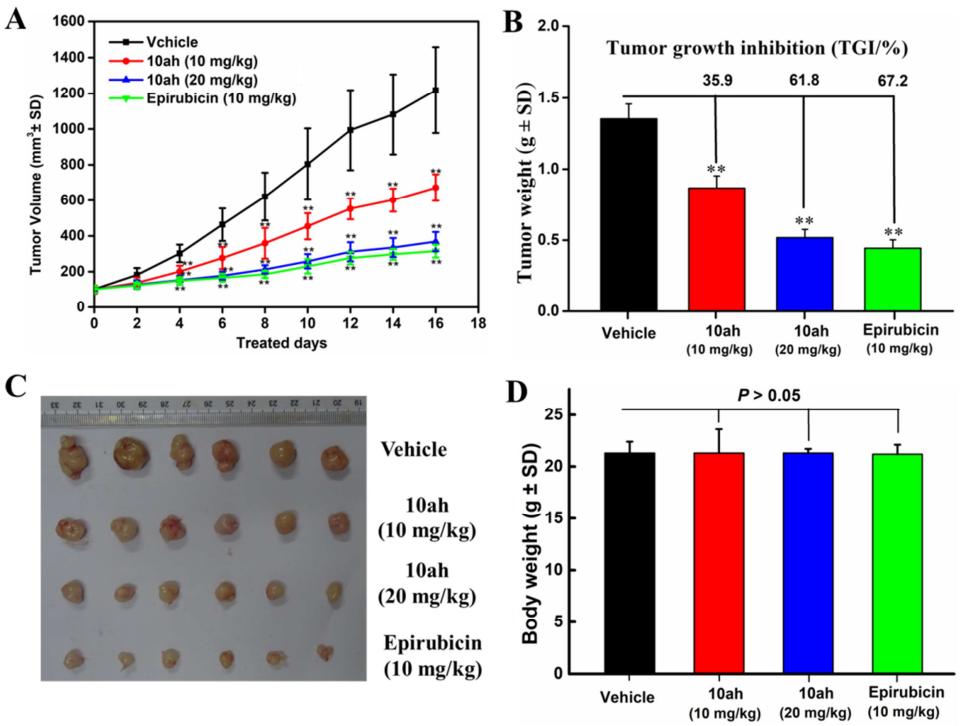

Fig. 6. The antitumor efficacy of **10ah** in human gastric carcinoma xenograft models *in vivo*. (A) Changes in tumor volume of mice from different groups over the observation period. (B) Tumor weight and tumor growth inhibition after treating with **10ah** at the end of treatment. (C) Photographs of excised tumor from vehicle group and treatment groups. (D) Body weight of mice at the end of treatment. Results are expressed as the mean ± SD, error bars represented SD, n = 6, (∗∗) $p < 0.01$ *vs* vehicle.

3. Conclusions

In this report, forty eight 2-styryl-4-aminoquinazolines derivatives as the analogue of CP-31398 were synthesized. Cytotoxicity evaluation identified the **10ah** as the most promising compound with IC_{50} values lowed to 1.73 μM against

MGC-803 cell lines. The molecular mechanism studies revealed that **10ah** and CP-31398 differ in their mode to interact with DNA and their mechanism on regulation p53 signal pathway, cell cycle and cell apoptosis to exert their tumor suppression activity. The study also revealed that **10ah** might exert its antitumor activity via intercalating into DNA, breaking the DNA double-strand to activate the p53 to cause cell cycle arrest, inducing fluctuation in the level of intracellular ROS, $Ca^{2+}$and MMP, up-regulating the pro-apoptosis proteins Bak, Bax and Bim while down-regulation the anti-apoptosis proteins Bcl-2 and Bcl-xL to mediate the intrinsic apoptosis. Furthermore, **10ah** also displayed promising anticancer efficiency *in vivo* with tumor growth inhibition (TGI) up to 61.8% without obvious toxicity. These results suggest that **10ah** may serve as a promising candidate in development of novel therapeutic agent to treat gastric cancer.

4. Experimental

4.1. General information

All chemicals employed in this work are commercially available and were used as received. Melting points were recorded on WRSIA apparatus and uncorrected. Thin layer chromatography (TLC) was performed on silica gel plates 60 F-254 and column chromatography on silica gel (200~300 mesh) from Branch of Qindao Marine Chemical Co., Ltd. NMR spectra were recorded in $CDCl_3$, CD_3OD and DMSO-d_6 on Bruker Advance (400 MHz, 500 MHz, 600 MHz) with TMS as internal standard. Chemical shifts were recorded in δ values. HRMS were measured in ESI mode and the mass analyzer of the HRMS was TOF.

4.2. Compounds synthesis and characterization

*4.2.1. General procedure for synthesis of **2***

Compound **1** (36.7 mmol) added to acetic anhydride (30 mL) and then stirred at

room temperature for 0.5 h (monitored by TLC, V_{EA}/V_{PE} = 1/2). After completion, 30 mL of water was added to the reaction mixture and precipitations occured. The precipitate was filtered off and washing successively with saturated $NaHCO_3$ and ethyl acetate to give white solid **2**.

2-Methyl-4-hydroxyquinazoline (**2a**). White solid, yield 67%, m.p. 174~176 □ (lit [35]. m.p. 176.5 °C); ^{1}H NMR (400 MHz, CD_3OD) δ 8.35 (d, J = 8.3 Hz, 1H), 7.72 (dd, J = 7.9, 1.4 Hz, 1H), 7.49~7.43 (m, 1H), 7.15~7.11 (m, 1H), 2.15 (s, 3H).

6-Chloro-2-methyl-4-hydroxyquinazoline (**2b**). White solid, yield 79%, m.p. 281~283 °C (lit [36]. m.p. 287 °C). ^{1}H NMR (400 MHz, $CDCl_3$) δ 10.96 (s, 1H), 8.61 (d, J = 8.9 Hz, 1H), 7.73~7.34 (m, 1H), 2.20 (s, 3H).

*4.2.2. General procedure for synthesis of **3~5***

The mixture of **2** (18.7 mmol) and aromatic aldehyde (22.5 mmol) in AcOH was stirred and refluxed for about 12 h (monitored by TLC, V_{EA}/V_{PE} = 1/2). After completion, 20 mL of water was added, the resultant precipitate was filtered off and washing successively with saturated $NaHCO_3$ and water to afford **3~5**.

(E)-2-(3,4-Dimethoxystyryl)-4-hydroxyquinazoline (**3a**). Pale yellow solid, yield 43%, m.p. 251~253 °C (lit [37]. m.p. 265~266 °C), ^{1}H NMR (500 MHz, DMSO-d_6) δ 12.21 (s, 1H), 8.10~8.09 (m, 1H), 7.89 (d, J = 16.1 Hz, 1H), 7.82~7.77 (m, 1H), 7.64 (d, J = 8.2 Hz, 1H), 7.47~7.44 (m, 1H), 7.28 (s, 1H), 7.23~7.17 (m, 1H), 7.03 (d, J = 8.2 Hz, 1H), 6.90 (d, J = 16.1 Hz, 1H), 3.84 (s, 3H), 3.81 (s, 3H).

(E)-2-(4-Nitrostyryl)-4-hydroxyquinazoline (**4a**). Yellow solid, yield 60%, m.p. 315~317 °C (lit [38]. m.p. >350 °C). ^{1}H NMR (400 MHz, DMSO-d_6) δ 12.44 (s, 1H), 8.30 (d, J = 8.6 Hz, 2H), 8.13 (d, J = 8.0 Hz, 1H), 8.04 (d, J = 16.2 Hz, 1H), 7.93 (d, J = 8.6 Hz, 2H), 7.86~7.82 (m, 1H), 7.71 (d, J = 8.0 Hz, 1H), 7.54~7.50 (m, 1H), 7.20 (d, J = 16.2 Hz, 1H).

(E)-2-(3,4-Methylenedioxystyryl)-4-hydroxyquinazoline (**5a**). Gray solid, yield 50%, m.p. 215~217 °C (lit [39]. m.p. 216~217 °C). ^{1}H NMR (400 MHz, DMSO-d_6) δ 8.09 (dd, J = 8.0, 1.5 Hz, 1H), 7.86 (d, J = 16.1 Hz, 1H), 7.81~7.77 (m, 1H), 7.64 (d, J = 8.1 Hz, 1H), 7.49~7.43 (m, 1H), 7.27 (d, J = 1.5 Hz, 1H), 7.15 (dd, J = 8.0, 1.5 Hz, 1H), 6.99 (d, J = 8.0 Hz, 1H), 6.84 (d, J = 16.1 Hz, 1H), 6.09 (s, 2H).

(E)-6-Chloro-2-(3,4-dimethoxystyryl)-4-hydroxyquinazoline (**3b**). Yellow solid, yield 37%, m.p. 294~296 °C. ^{1}H NMR (400 MHz, DMSO-d_6) δ 12.36 (s, 1H), 8.02 (s, 1H), 7.90 (d, J = 16.1 Hz, 1H), 7.81 (d, J = 8.6 Hz, 1H), 7.65 (d, J = 8.6 Hz, 1H), 7.26 (s, 1H), 7.20 (d, J = 8.3 Hz, 1H), 7.03 (d, J = 8.3 Hz, 1H), 6.88 (d, J = 16.1 Hz, 1H), 3.83 (s, 3H), 3.81 (s, 3H).

(*E*)*-6-Chloro-2-(4-nitrostyryl)-4-hydroxyquinazoline* (**4b**). Yellow solid, yield 49%, m.p. 352~355 °C. ^{1}H NMR (400 MHz, DMSO-d_6) δ 12.57 (s, 1H), 8.27 (d, J = 8.8 Hz, 2H), 8.06~7.97 (m, 2H), 7.89 (d, J = 8.8 Hz, 2H), 7.83(dd, J = 8.7, 2.5 Hz 1H), 7.70 (d, J = 8.7 Hz, 1H), 7.16 (d, J = 16.2 Hz, 1H). ^{13}C NMR (100 MHz, DMSO-d_6) δ 161.1, 151.7, 148.1, 148.0, 141.8, 136.7, 135.2, 131.4, 130.0, 129.1, 125.6, 125.4, 124.7, 123.0.

(E)-6-Chloro-2-(3,4-methylenedioxystyryl)-4-hydroxyquinazoline (**5b**). Yellow solid, yield 39%, m.p. 357~359 °C. ^{1}H NMR (400 MHz, DMSO-d_6) δ 7.95 (d, J = 2.5 Hz, 1H), 7.75 (d, J = 16.0 Hz, 1H), 7.61 (dd, J = 8.7, 2.5 Hz, 1H), 7.52 (d, J = 8.7 Hz, 1H), 7.27 (d, J = 1.5 Hz, 1H), 7.11 (dd, J = 8.0, 1.5 Hz, 1H), 6.97 (d, J = 8.0 Hz, 1H), 6.82 (d, J = 16.0 Hz, 1H), 6.06 (s, 2H) (the resonance of O−H was not observed in DMSO-d_6).

*4.2.3. General procedure for synthesis of **6~8***

The mixture of **3~5** (6.5 mmol), $POCl_3$ (32.4 mmol), *N*,*N*-dimethylaniline in toluene was stirred and refluxed for 10 h (monitored by TLC, V_{EA}/V_{PE} = 1/2). After completion, the solvent was removed under reduced pressure and the residue was purified on silica gel to provide **6~8**.

(E)-4-Chloro-2-(3,4-dimethoxystyryl)quinazoline (**6a**). Yellow solid, yield 76%, m.p. 167~169 □.

(E)-4-Chloro-2-(4-nitrostyryl)quinazoline (**7a**). Yellow solid, yield 94%, m.p. 154~156 □.

(E)-4-Chloro-2-(3,4-Methylenedioxystyryl)quinazoline (**8a**). reddish-brown solid, yield 90%, m.p. 105–107 □.

(E)-4,6-Dichloro-2-(3,4-dimethoxystyryl)quinazoline (**6b**). Yellow solid, 44% yield, m.p. 165~167 □.

(E)-4,6-Dichloro-2-(4-nitrostyryl)quinazoline (**7b**). Gray solid, 51% yield, m.p. 173~175 □.

(E)-2-(3,4-Methylenedioxystyryl)-4,6-dichloroquinazoline (**8b**). Yellow solid, 94% yield, m.p. 236~238 □.

These products hardly dissolved in the common solvents and can't be further structurally characterized by NMR.

*4.2.4. General procedure for synthesis of **9~11***

The mixture of **6~8** (1.4 mmol), DMAP (0.3 mmol), TEA, amine (0.5 mmol) in toluene was stirred and refluxed for 12 h (monitored by TLC, V_{MeOH}/V_{DCM} = 1/10). The solvent was evaporated under reduced pressure when the reaction was completed, and the residue was purified by column chromatography on silica gel (V_{MeOH}/V_{DCM} = 1/20) to afford **9~11**. The structures were confirmed by NMR and HRMS.

(E)-2-(3,4-Dimethoxystyryl)-4-(2-dimethylaminoethyl)aminoquinazoline (**9aa**). Yellow solid, yield 31%, m.p. 154~156 °C. ^{1}H NMR (400 MHz, $CDCl_3$) δ 7.96 (d, J = 15.7 Hz, 1H), 7.79 (d, J = 8.2 Hz, 1H), 7.72 (d, J = 8.2 Hz, 1H), 7.70~7.66 (m, 1H), 7.40~7.36 (m, 1H), 7.23 (d, J=1.4 Hz, 1H), 7.16 (dd, J=8.2, 1.4 Hz, 1H), 7.11 (d, J = 15.7 Hz, 1H), 6.87 (d, J = 8.2 Hz, 1H), 6.52 (s,1H), 3.93 (s, 3H), 3.90 (s, 3H), 3.82~3.76 (m, 2H), 2.66 (t, J = 5.8 Hz, 2H), 2.33 (s, 6H). ^{13}C NMR (100 MHz, $CDCl_3$) δ 161.1, 159.1, 150.3, 149.7, 149.1, 136.8, 132.5, 129.8, 128.1, 127.3, 125.1, 121.6, 121.0, 114.0, 111.1, 109.2, 57.6, 55.9, 55.8, 45.3, 38.2. HRMS (ESI) *m/z* calcd for $C_{22}H_{27}N_4O_2$ $[M+H]^+$ 379.2129, found 379.2119.

(E)-2-(3,4-Dimethoxystyryl)-4-(2-diethylaminoethyl)aminoquinazoline (**9ab**). Yellow solid, yield 35%, m.p. 141~143 °C. ^{1}H NMR (500 MHz, $CDCl_3$) δ 7.97 (d, J = 15.7 Hz, 1H), 7.79 (d, J = 8.3 Hz, 1H), 7.70~7.67 (m, 2H), 7.41~7.37 (m, 1H), 7.24 (d, J = 1.7 Hz, 1H), 7.16 (dd, J = 8.3, 1.7 Hz, 1H), 7.11 (d, J = 15.7 Hz, 1H), 6.88 (d, J = 8.3 Hz, 1H), 6.72 (s, 1H), 3.93 (s, 3H), 3.91 (s, 3H), 3.80~3.76 (m, 2H), 2.81 (t, J = 6.0 Hz, 2H), 2.65 (q, J = 7.1 Hz, 4H), 1.10 (t, J = 7.1 Hz, 6H). ^{13}C NMR (100 MHz, $CDCl_3$) δ 161.1, 159.0, 150.2, 149.7, 149.1, 136.7, 132.4, 129.8, 128.1, 127.3, 125.2, 121.5, 120.8, 114.1, 111.0, 109.1, 55.9, 55.8, 51.1, 46.8, 38.1, 12.0. HRMS (ESI) *m/z*

calcd for $C_{24}H_{31}N_4O_2$ $[M+H]^+$ 407.2442, found 407.2433.

(E)-2-(3,4-Dimethoxystyryl)-4-(2-diisopropylaminoethyl)aminoquinazoline (**9ac**). Gray solid, yield 25%, m.p. 124~126 °C. ^{1}H NMR (500 MHz, $CDCl_3$) δ 7.96 (d, J = 15.7 Hz, 1H), 7.79 (d, J = 8.3 Hz, 1H), 7.69~7.65 (m, 2H), 7.39~7.36 (m, 1H), 7.23 (s, 1H), 7.16 (d, J = 8.3 Hz, 1H), 7.10 (d, J = 15.7 Hz, 1H), 6.87 (d, J = 8.3 Hz, 1H), 3.93 (s, 3H), 3.90 (s, 3H), 3.75~3.69 (m, 2H), 3.18~3.12 (m, 2H), 2.86 (t, J = 5.4 Hz, 2H), 1.10 (d, J = 6.6 Hz, 12H). ^{13}C NMR (125 MHz, $CDCl_3$) δ 161.1, 158.9, 150.2, 149.7, 149.1, 136.7, 132.3, 129.8, 128.1, 127.3, 125.1, 121.5, 120.6, 114.1, 111.1, 109.2, 55.9, 55.8, 38.8, 20.8. HRMS (ESI) *m/z* calcd for $C_{26}H_{35}N_4O_2$ $[M+H]^+$ 435.2755, found 435.2747 (the resonance of O-H was not observed in $CDCl_3$).

(E)-2-(3,4-dimethoxystyryl)-4-(1-piperidinylethyl)aminoquinazoline (**9ad**). Yellow solid, yield 43%, m.p. 127~129 °C. ^{1}H NMR (400 MHz, $CDCl_3$) δ 7.96 (d, J = 15.7 Hz, 1H), 7.79 (d, J = 7.9 Hz, 1H), 7.75~7.65 (m, 2H), 7.43~7.35 (m, 1H), 7.23 (d, J = 1.8 Hz, 1H), 7.16 (dd, J = 8.3, 1.8 Hz, 1H), 7.10 (d, J = 15.7 Hz, 1H), 6.87 (d, J = 8.3 Hz, 1H), 6.78 (s, 1H), 3.93 (s, 3H), 3.91 (s, 3H), 3.82~3.79 (m, 2H), 2.71 (t, J = 6.0 Hz, 2H), 2.57~2.46 (m, 4H), 1.68~1.61 (m, 4H), 1.54~1.46 (m, 2H). ^{13}C NMR (100 MHz, $CDCl_3$) δ 161.1, 159.0, 150.2, 149.7, 149.1, 136.8, 132.4, 129.8, 128.1, 127.3, 125.1, 121.6, 120.8, 114.1, 111.0, 109.1, 56.7, 55.9, 55.8, 54.2, 37.3, 26.2, 24.4. HRMS (ESI) *m/z* calcd for $C_{25}H_{31}N_4O_2$ $[M+H]^+$ 419.2442, found 419.2434.

(E)-2-(3,4-Dimethoxystyryl)-4-[2-(morpholinyl)ethyl]-aminoquinazoline (**9ae**). Yellow solid, yield 38%, m.p. 145~147 °C. ^{1}H NMR (400 MHz, $CDCl_3$) δ 7.96 (d, J = 15.7 Hz, 1H), 7.81 (d, J = 8.2 Hz, 1H), 7.72~7.67 (m, 2H), 7.43~7.39 (m, 1H), 7.23 (d, J = 1.7 Hz, 1H), 7.15 (dd, J = 8.2, 1.7 Hz, 1H), 7.11 (d, J = 15.7 Hz, 1H), 6.87 (d, J = 8.2 Hz, 1H), 6.52 (s, 1H), 3.93 (s, 6H), 3.86~3.81 (m, 2H), 3.79~3.75 (m, 4H), 2.76 (t, J = 6.0 Hz, 2H), 2.60~2.55 (m, 4H). ^{13}C NMR (100 MHz, $CDCl_3$) δ 161.1, 159.0, 150.2, 149.8, 149.2, 137.0, 132.6, 129.7, 128.2, 127.2, 125.3, 121.6, 120.7, 113.9, 111.1, 109.1, 67.1, 56.7, 55.9, 55.8, 53.4, 37.0. HRMS (ESI) *m/z* calcd for $C_{24}H_{29}N_4O_3$ $[M+H]^+$ 421.2234, found 421.2224.

(E)-2-(3,4-Dimethoxystyryl)-4-(3-dimethylaminopropyl)aminoquinazoline (**9af**). Yellow solid, yield 33%, m.p. 172~174 °C. ^{1}H NMR (400 MHz, CD_3OD) δ 8.20~8.18

(m, 1H), 8.09 (d, *J* = 15.6 Hz, 1H), 7.86~7.81 (m, 1H), 7.69 (d, *J* = 8.0 Hz, 1H), 7.57~7.53 (m, 1H), 7.30~7.25 (m, 2H), 7.00~6.95 (m, 2H), 3.96 (t, *J* = 6.7 Hz, 2H), 3.89 (s, 3H), 3.86 (s, 3H), 3.65~3.55 (m, 2H), 2.89 (s, 6H), 2.28~2.24 (m, 2H). ^{13}C NMR (100 MHz, CD_3OD) δ 160.1, 158.8, 151.4, 149.4, 143.6, 142.0, 134.3, 128.2, 126.6, 122.9, 122.5, 122.2, 120.0, 113.0, 111.4, 110.3, 55.4, 55.2, 55.1, 42.2, 38.1, 24.3. HRMS (ESI) *m/z* calcd for $C_{23}H_{29}N_4O_2$ $[M+H]^+$ 393.2285, found 393.2274.

(E)-2-(3,4-Dimethoxystyryl)-4-(3-diethylaminopropyl)aminoquinazoline (**9ag**). Yellow sticky solid. This compound deteriorates easily and can't be further structurally characterized by NMR. HRMS (ESI) *m/z* calcd for $C_{25}H_{33}N_4O_2$ $[M+H]^+$ 421.2598, found 421.2592.

(E)-2-(3,4-Dimethoxystyryl)-4-(4-aminobutyl)aminoquinazoline (**9ah**). Yellow solid, yield 41%, m.p. 177~179 °C. ^{1}H NMR (400 MHz, CD_3OD) δ 8.03 (dd, *J* = 8.1, 3.9 Hz, 1H), 7.97~7.86 (m, 1H), 7.71~7.63 (m, 2H), 7.45~7.35 (m, 1H), 7.30~7.09 (m, 2H), 7.00~6.91 (m, 2H), 3.93 (s, 3H), 3.87 (s, 3H), 3.80~3.75 (m, 2H), 2.88~2.84 (m, 2H), 1.89~1.82 (m, 2H), 1.77~1.62 (m, 2H). ^{13}C NMR (100 MHz, CD_3OD) δ 161.0, 159.7, 150.3, 149.3, 137.6, 135.4, 132.5, 129.5, 126.0, 125.4, 125.1, 121.9, 121.4, 113.9, 111.4, 109.8, 55.1, 55.0, 40.2, 40.0, 27.4, 26.1. HRMS (ESI) *m/z* calcd for $C_{22}H_{27}N_4O_2$ $[M+H]^+$ 379.2129, found 379.2125.

(E)-2-(4-Nitrostyryl)-4-(2-dimethylaminoethyl)aminoquinazoline (**10aa**). Yellow solid, yield 45%, m.p. 156~158 °C. ^{1}H NMR (400 MHz, $CDCl_3$) δ 8.23 (d, *J* = 8.6 Hz, 2H), 8.02 (d, *J* = 15.8 Hz, 1H), 7.83 (d, *J* = 8.3 Hz, 1H), 7.79 (d, *J* = 8.2 Hz, 1H), 7.76~7.69 (m, 3H), 7.48~7.43 (m, 1H), 7.34 (d, *J* = 15.8 Hz, 1H), 6.68 (s, 1H), 3.82~3.77 (m, 2H), 2.71~2.67 (m, 2H), 2.35 (s, 6H). ^{13}C NMR (125MHz, $CDCl_3$) δ 159.9, 150.0, 147.3, 143.2, 134.1, 133.8, 132.8, 129.2, 128.4, 127.9, 125.9, 124.1, 121.1, 114.2, 57.5, 45.2, 38.2. HRMS (ESI) *m/z* calcd for $C_{20}H_{22}N_5O_2$ $[M+H]^+$ 364.1768, found 364.1751.

(E)-2-(4-Nitrostyryl)-4-(2-diethylaminoethyl)aminoquinazoline (**10ab**). Brown solid, yield 59%, m.p. 151~153 °C. ^{1}H NMR (400 MHz, $CDCl_3$) δ 8.23 (d, *J* = 8.8 Hz, 2H), 8.03 (d, *J* = 15.8 Hz, 1H), 7.83 (d, *J* = 8.3 Hz, 1H), 7.76~7.69 (m, 4H), 7.48~7.43 (m, 1H), 7.34 (d, *J* = 15.8 Hz, 1H), 6.83 (s, 1H), 3.79~3.74 (m, 2H),

2.84~2.80 (m, 2H), 2.66 (q, *J* = 7.1 Hz, 4H), 1.11 (t, *J* = 7.1 Hz, 6H). ^{13}C NMR (100 MHz, $CDCl_3$) δ 159.9, 159.1, 149.9, 147.2, 143.1, 134.0, 133.7, 132.6, 128.3, 127.8, 125.9, 124.0, 120.8, 114.2, 51.0, 46.7, 38.1, 12.0. HRMS (ESI) *m/z* calcd for $C_{22}H_{26}N_5O_2$ $[M+H]^+$ 392.2081, found 392.2072.

(E)-2-(4-Nitrostyryl)-4-(2-diisopropylaminoethyl)aminoquinazoline (**10ac**). Yellow solid, yield 45%, m.p. 214~216 °C. ^{1}H NMR (400 MHz, $CDCl_3$) δ 8.68 (s, 1H), 8.28 (d, *J* = 8.0 Hz, 1H), 8.21 (d, *J* = 8.8 Hz, 2H), 7.91 (d, *J* = 15.9 Hz, 1H), 7.79 (d, *J* = 7.8 Hz, 1H), 7.73~7.70 (m, 3H), 7.53~7.45 (m, 1H), 7.32 (d, *J* = 15.9 Hz, 1H), 4.29~4.21 (m, 2H), 3.64~3.55 (m, 2H), 3.36~3.29 (m, 2H), 1.41 (d, *J* = 5.6 Hz, 12H). ^{13}C NMR (100 MHz, $CDCl_3$) δ 159.4, 159.2, 150.0, 147.4, 143.1, 133.8, 133.7, 133.2, 127.9, 127.8, 126.9, 124.1, 122.8, 114.4, 55.7, 47.3, 38.3, 18.8. HRMS (ESI) *m/z* calcd for $C_{24}H_{30}N_5O_2$ $[M+H]^+$ 420.2394, found 420.2386.

(E)-2-(4-Nitrostyryl)-4-(1-piperidinylethyl)aminoquinazoline (**10ad**). Yellow solid, yield 38%, m.p. 166~168 °C. ^{1}H NMR (500 MHz, $CDCl_3$) δ 8.22 (d, *J* = 8.8 Hz, 2H), 8.01 (d, *J* = 15.9 Hz, 1H), 7.82 (d, *J* = 8.0 Hz, 1H), 7.75~7.70 (m, 4H), 7.49~7.44 (m, 1H), 7.33 (d, *J* = 15.9 Hz, 1H), 6.82 (s, 1H), 3.80~3.76 (m, 2H), 2.71 (t, *J* = 6.0 Hz, 2H), 2.55~2.47 (m, 4H), 1.68~1.62 (m, 4H), 1.54~1.48 (s, 2H). ^{13}C NMR (125 MHz, $CDCl_3$) δ 160.0, 159.1, 150.1, 147.4, 143.2, 134.1, 133.9, 132.6, 128.5, 127.9, 126.0, 124.1, 120.9, 114.3, 56.3, 54.3, 37.4, 26.2, 24.4. HRMS (ESI) *m/z* calcd for $C_{23}H_{26}N_5O_2$ $[M+H]^+$ 404.2081, found 404.2075.

(E)-2-(4-Nitrostyryl)-4-[2-(morpholinyl)ethyl]-aminoquinazoline (**10ae**). Yellow solid, yield 41%, m.p. 189~191 °C. ^{1}H NMR (400 MHz, $CDCl_3$) δ 8.21 (d, *J* = 8.8 Hz, 2H), 8.00 (d, *J* = 15.9 Hz, 1H), 7.84 (d, *J* = 7.9 Hz, 1H), 7.79~7.66 (m, 4H), 7.51~7.43 (m, 1H), 7.33 (d, *J* = 15.9 Hz, 1H), 6.60 (s, 1H), 3.85~3.76 (m, 6H), 2.78 (t, *J* = 6.0 Hz, 2H), 2.61~2.56 (m, 4H). ^{13}C NMR (100 MHz, $CDCl_3$) δ 159.8, 159.1, 150.0, 147.3, 143.1, 134.1, 133.6, 132.7, 128.5, 127.8, 126.0, 124.0, 120.7, 114.1, 67.0, 56.5, 53.3, 36.9. HRMS (ESI) *m/z* calcd for $C_{22}H_{24}N_5O_3$ $[M+H]^+$ 406.1874, found 406.1869.

(E)-2-(4-Nitrostyryl)-4-(3-dimethylaminopropyl)aminoquinazoline (**10af**). Yellow solid, yield 58%, m.p. 161~163 °C. ^{1}H NMR (500 MHz, $CDCl_3$) δ 8.62 (s,

1H), 8.33 (d, *J* = 8.2 Hz,1H), 8.23 (d, *J* = 8.0 Hz, 2H), 8.06~8.01 (m, 3H), 7.79~7.74 (d, *J* = 7.0 Hz, 1H), 7.71 (d, *J* = 8.3 Hz, 1H), 7.52~7.48 (m, 1H), 7.37 (d, *J* = 16.0 Hz, 1H), 3.79~3.74 (m, 2H), 3.21~3.17 (m, 2H), 2.75 (s, 6H), 2.17~2.11 (m, 2H). ^{13}C NMR (125 MHz, $CDCl_3$) δ 164.5, 164.5, 164.4, 154.8, 152.1, 148.1, 139.1, 138.9, 138.0, 133.7, 132.7, 129.2, 128.2, 119.3, 59.9, 47.3, 42.9, 29.0. HRMS (ESI) *m/z* calcd for $C_{21}H_{24}N_5O_2$ $[M+H]^+$ 378.1925, found 378.1921.

(E)-2-(4-Nitrostyryl)-4-(3-diethylaminopropyl)aminoquinazoline (**10ag**). Yellow solid, yield 31%, m.p. 130~132 °C. ^{1}H NMR (600 MHz, $CDCl_3$) δ 8.90 (s, 1H), 8.21 (d, *J* = 8.7 Hz, 2H), 7.99 (d, *J* = 15.8 Hz, 1H), 7.82~7.77 (m, 2H), 7.73 (d, *J* = 8.7 Hz, 2H), 7.70~7.67 (m, 1H), 7.43~7.39 (m, 1H), 7.32 (d, *J* = 15.8 Hz, 1H), 3.88~8.85 (m, 2H), 2.83~2.79 (m, 2H), 2.76 (q, *J* = 7.1 Hz, 4H), 2.01~1.96 (m, 2H), 1.17 (t, *J* = 7.1 Hz, 6H). ^{13}C NMR (150 MHz, $CDCl_3$) δ 160.0, 159.4, 149.9, 147.2, 143.3, 134.0, 133.8, 132.5, 128.1, 127.8, 125.7, 124.0, 121.7, 114.5, 52.9, 46.8, 41.9, 24.0, 10.9. HRMS (ESI) *m/z* calcd for $C_{23}H_{28}N_5O_2$ $[M+H]^+$ 406.2238, found 406.2231.

(E)-2-(4-Nitrostyryl)-4-(4-aminobutyl)aminoquinazoline (**10ah**). Yellow solid, yield 57%, m.p. 172~174 °C, ^{1}H NMR (400 MHz, CD_3OD) δ 8.08 (d, *J* = 8.8 Hz, 2H), 7.98 (d, *J* = 7.7 Hz, 1H), 7.89 (d, *J* = 15.8 Hz, 1H), 7.71~7.61 (m, 4H), 7.42~7.38 (m, 1H), 7.13 (d, *J* = 15.8 Hz, 1H), 3.76~3.71 (m, 2H), 2. 87~2.82 (m, 2H), 1.87~1.78 (m, 2H), 1.74~1.66 (m, 2H). ^{13}C NMR (100 MHz, CD_3OD) δ 159.8, 159.6, 149.1, 147.4, 142.6, 134.7, 132.6, 131.9, 127.7, 126.3, 125.8, 123.5, 122.0, 114.1, 40.3, 40.2, 27.8, 26.0. HRMS (ESI) *m/z* calcd for $C_{20}H_{22}N_5O_2$ $[M+H]^+$ 364.1768, found 364.1761 (the resonance of O−H and H−N−H were not observed in CD_3OD).

(E)-2-(3,4-Methylenedioxystyryl)-4-(2-dimethylaminoethyl)aminoquinazoline (**11aa**). Yellow solid, yield 45%, m.p. 156~158 °C. ^{1}H NMR (500 MHz, DMSO-d_6) δ 8.33 (s, 1H), 8.24 (d, *J* = 8.2 Hz, 1H), 7.87 (d, *J* = 15.8 Hz, 1H), 7.75~7.71 (m, 1H), 7.67 (d, *J* = 8.2 Hz, 1H), 7.47~7.42 (m, 1H), 7.40~7.38 (m, 1H), 7.14 (d, *J* = 8.0 Hz, 1H), 7.02 (d, *J* = 15.8 Hz, 1H), 6.96 (d, *J* = 8.0 Hz, 1H), 6.08 (s, 2H), 3.87~3.83 (m, 2H), 2.92~2.86 (m, 2H), 2.50 (s, 6H). ^{13}C NMR (125 MHz, DMSO-d_6) δ 160.6, 159.5, 150.4, 148.5, 148.4, 136.5, 133.0, 131.1, 127.9, 127.8, 125.4, 123.5, 123.3, 114.4,

108.9, 106.6, 101.7, 57.4, 44.8, 26.8. HRMS (ESI) *m/z* calcd for $C_{21}H_{23}N_4O_2$ $[M+H]^+$ 363.1816, found 363.1816.

(E)-2-(3,4-Methylenedioxystyryl)-4-(2-diethylaminoethyl)aminoquinazoline (**11ab**). Yellow solid, yield 30%, m.p. 141~143 °C. ^{1}H NMR (400 MHz, $CDCl_3$) δ 7.90 (d, J = 15.8 Hz, 1H), 7.82~7.77 (m, 2H), 7.68~7.64 (m, 1H), 7.40~7.36 (m, 1H), 7.16 (d, J = 1.5 Hz, 1H), 7.07~7.02 (m, 2H), 6.80 (d, J = 8.0 Hz, 1H), 5.97 (s, 2H), 3.83 (t, J = 5.6 Hz, 2H), 3.38 (s, 1H), 2.92~2.86 (m, 2H), 2.72 (q, J = 7.2 Hz, 4H), 1.13 (t, J = 7.2 Hz, 6H). ^{13}C NMR (100 MHz, $CDCl_3$) δ 161.1, 159.0, 150.3, 148.2, 148.1, 136.6, 132.4, 131.3, 128.2, 127.6, 125.2, 123.0, 120.7, 114.1, 108.4, 106.4, 101.2, 77.3, 77.0, 76.7, 51.1, 46.8, 38.1, 12.1. HRMS (ESI) *m/z* calcd for $C_{23}H_{27}N_4O_2$ $[M+H]^+$ 391.2129, found 391.2129.

(E)-2-(3,4-Methylenedioxystyryl)-4-(2-diisopropylaminoethyl)aminoquinazoline (**11ac**). Yellow solid, yield 60%, m.p. 169~171 °C. ^{1}H NMR (400 MHz, $CDCl_3$) δ 7.93 (d, J = 15.8 Hz, 1H), 7.79 (d, J = 7.9 Hz, 1H), 7.70~7.65 (m, 2H), 7.41~7.36 (m, 1H), 7.18 (d, J = 1.6 Hz, 1H), 7.10~7.03 (m, 2H), 6.82 (d, J = 7.9 Hz, 1H), 5.99 (m, 2H), 3.80~3.65 (m, 2H), 3.25~3.10 (m, 2H), 2.95~2.75 (m, 2H), 1.12 (d, J = 5.4 Hz, 12H). ^{13}C NMR (100 MHz, $CDCl_3$) δ 161.1, 159.0, 150.3, 148.2, 148.1, 136.6, 132.4, 131.3, 128.2, 127.6, 125.3, 123.0, 120.7, 114.2, 108.4, 106.4, 101.2, 47.7, 42.7, 38.7, 29.7, 20.8. HRMS (ESI) *m/z* calcd for $C_{25}H_{31}N_4O_2$ $[M+H]^+$ 419.2442, found 419.2434 (the resonance of O-H was not observed in $CDCl_3$).

(E)-2-(3,4-Methylenedioxystyryl)-4-(1-piperidinylethyl)aminoquinazoline (**11ad**). Yellow solid, yield 29%. m.p, 169~171 °C. ^{1}H NMR (400 MHz, $CDCl_3$) δ 7.92 (d, J = 15.7 Hz, 1H), 7.78 (dd, J = 8.3, 0.7 Hz, 1H), 7.74 (dd, J = 8.3, 0.7 Hz, 1H), 7.68~7.64 (m, 1H), 7.39~7.35 (m, 1H), 7.17 (d, J = 1.6 Hz, 1H), 7.08~7.02 (m, 2H), 6.85 (s, 1H), 6.80 (d, J = 8.0 Hz, 1H), 5.97 (s, 2H), 3.82~3.77 (m, 2H), 2.71~2.67 (m, 2H), 2.53~2.45 (m, 4H), 1.67~1.60 (m, 4H), 1.52~1.45 (m, 2H). ^{13}C NMR (100 MHz, $CDCl_3$) δ 161.0, 159.0, 150.1, 148.1, 148.1, 136.7, 132.4, 131.2, 128.0, 127.4, 125.1, 122.9, 121.1, 114.1, 108.4, 106.3, 101.2, 56.9, 54.2, 37.3, 26.0, 24.3. HRMS (ESI) *m/z* calcd for $C_{24}H_{27}N_4O_2$ $[M+H]^+$ 403.2129, found 403.2129.

(E)-2-(3,4-Methylenedioxystyryl)-4-[2-(morpholinyl)ethyl]-aminoquinazoline

(**11ae**). Yellow solid, yield 38%, m.p. 245~247 °C. ^{1}H NMR (400 MHz, $CDCl_3$) δ 7.93 (d, J = 15.7 Hz, 1H), 7.81 (d, J = 8.3 Hz, 1H), 7.72~7.66 (m, 2H), 7.43~7.37 (m, 1H), 7.17 (d, J = 1.6 Hz, 1H), 7.08~7.03 (m, 2H), 6.81 (d, J = 8.0 Hz, 1H), 6.54 (s, 1H), 5.98 (s, 2H), 3.85~3.79 (m, 2H), 3.77 (t, J = 4.4 Hz, 4H), 2.75 (t, J = 5.9 Hz, 2H), 2.60~2.54 (m, 4H). ^{13}C NMR (100 MHz, $CDCl_3$) δ 160.9, 159.0, 150.1, 148.2, 136.9, 132.5, 131.1, 128.1, 127.2, 125.2, 123.0, 120.7, 113.9, 108.4, 106.3, 101.2, 67.0, 56.6, 53.3, 36.9. HRMS (ESI) *m/z* calcd for $C_{23}H_{25}N_4O_2$ $[M+H]^+$ 405.1921, found 405.1918.

(E)-2-(3,4-Methylenedioxystyryl)-4-(3-dimethylaminopropyl)aminoquinazoline (**11af**). White solid, yield 43%, m.p. 133~135 °C. ^{1}H NMR (500 MHz, $CDCl_3$) δ 8.55 (s, 1H) , 7.95 (d, J = 15.7 Hz, 1H), 7.79 (d, J = 8.0 Hz, 1H), 7.67 (t, J = 7.5 Hz, 1H), 7.59 (d, J= 8.0 Hz, 1H), 7.37 (t, J = 7.5 Hz, 1H), 7.20 (s, 1H), 7.11~7.06 (m, 2H), 6.83 (d, J = 7.5 Hz, 1H), 6.00 (s, 2H), 3.86 (d, J = 4.4 Hz, 2H), 2.60 (d, J = 4.8 Hz, 2H), 2.38 (s, 6H), 1.91 (s, 2H). ^{13}C NMR (125 MHz, $CDCl_3$) δ 161.2, 159.3, 150.2, 148.3, 148.2, 136.5, 132.2, 131.3, 128.0, 127.7, 125.0, 123.0, 121.1, 114.4, 108.4, 106.4, 101.2, 59.9, 45.6, 42.3, 24.9. HRMS (ESI) *m/z* calcd for $C_{22}H_{25}N_4O_2$ $[M+H]^+$ 377.1972, found 377.1967.

(E)-2-(3,4-Methylenedioxystyryl)-4-(3-diethylaminopropyl)aminoquinazoline (**11ag**). Yellow solid, yield 49%, m.p. 161~163 °C. ^{1}H NMR (400 MHz, $CDCl_3$) δ 8.75 (s, 1H), 7.93 (d, J = 15.7 Hz, 1H), 7.77 (d, J = 8.2 Hz, 1H), 7.67~7.63 (m, 2H), 7.38~7.31 (m, 1H), 7.18 (d, J = 1.5 Hz, 1H), 7.08 (dd, J = 8.1, 1.5 Hz, 1H), 7.05 (d, J = 15.7 Hz, 1H), 6.81 (d, J = 8.1 Hz, 1H), 5.98 (s, 2H), 3.87~3.83 (m, 2H), 2.74~2.71 (m, 2H), 2.67 (q, J = 7.1 Hz, 4H), 1.93~1.87 (m, 2H), 1.12 (t, J = 7.1 Hz, 6H). ^{13}C NMR (100 MHz, $CDCl_3$) δ 161.1, 159.2, 150.2, 148.2, 148.1, 136.5, 132.2, 131.3, 128.0, 127.7, 124.8, 122.9, 121.4, 114.4, 108.4, 106.4, 101.2, 53.6, 47.1, 42.7, 24.5, 11.5. HRMS (ESI) *m/z* calcd for $C_{24}H_{29}N_4O_2$ $[M+H]^+$ 405.2285, found 405.2278.

(E)-2-(3,4-Methylenedioxystyryl)-4-(4-aminobutyl)aminoquinazoline (**11ah**). Yellow solid, yield 31%, m.p. 182~184 °C. ^{1}H NMR (400 MHz, CD_3OD) δ: 8.18 (d, J = 7.8 Hz, 1H), 8.02 (d, J = 15.5 Hz, 1H), 7.84~7.80 (m, 1H), 7.67 (d, J = 8.2 Hz, 1H), 7.56~7.52 (m, 1H), 7.20 (d, J = 1.4 Hz, 1H), 7.14 (dd, J = 8.0, 1.4 Hz, 1H), 6.90 (d, J

= 15.5 Hz, 2H), 6.84(d, *J*= 8.0 Hz, 2H), 6.00 (s, 2H), 3.88 (t, *J* = 6.6 Hz, 2H), 3.04~3.00 (m, 2H), 1.93~1.86 (m, 2H), 1.84~1.79 (m, 2H). HRMS (ESI) *m/z* calcd for $C_{21}H_{23}N_4O_2$ $[M+H]^+$ 363.1816, found 363.1809. Because of its poor solubility, compound **11ah** could not be characterized by ^{13}C NMR.

(E)-6-Chloro-2-(3,4-dimethoxystyryl)-4-(2-dimethylaminoethyl)aminoquinazoline (**9ba**). Yellow solid, yield 48%, m.p. 170~171 °C. ^1H NMR (400 MHz, $CDCl_3$) δ 7.95 (d, *J* = 15.7 Hz, 1H), 7.74~7.70 (m, 2H), 7.63~7.60 (m, 1H), 7.22 (d, *J* = 1.8 Hz, 1H), 7.16 (dd, *J* = 8.3, 1.8 Hz, 1H), 7.07 (d, *J* = 15.7 Hz, 1H), 6.88 (d, *J* = 8.3 Hz, 1H), 6.48 (s, 1H), 3.94 (s, 3H), 3.91 (s, 3H), 3.82~3.77 (m, 2H), 2.70~2.66 (m, 2H), 2.35 (s, 6H). ^{13}C NMR (100 MHz, $CDCl_3$) δ 161.3, 158.2, 149.9, 149.2, 148.9, 137.3, 133.2, 130.3, 129.8, 129.6, 126.9, 121.7, 120.6, 114.7, 111.1, 109.2, 57.5, 55.9, 55.9, 45.2, 38.3. HRMS (ESI) *m/z* calcd for $C_{22}H_{26}ClN_4O_2$ $[M+H]^+$ 413.1739, found 413.1735.

(E)-6-Chloro-2-(3,4-dimethoxystyryl)-4-(2-diethylaminoethyl)aminoquinazoline (**9bb**). Yellow solid, yield 35%, m.p. 133~135 °C. ^1H NMR (400 MHz, $CDCl_3$) δ 7.95 (d, *J* = 15.7 Hz, 1H), 7.72 (d, *J* = 8.7 Hz, 1H), 7.64~7.60 (m, 2H), 7.22 (d, *J* = 1.7 Hz, 1H), 7.16 (dd, *J* = 8.3, 1.7 Hz, 1H), 7.07 (d, *J* = 15.7 Hz, 1H), 6.88 (d, *J* = 8.3 Hz, 1H), 6.64 (s, 1H), 3.93 (s, 3H), 3.91 (s, 3H), 3.79~3.74 (m, 2H), 2.81 (t, *J* = 5.9 Hz, 2H), 2.66 (q, *J* = 7.1 Hz, 4H), 1.11 (t, *J* = 7.1 Hz, 6H). ^{13}C NMR (100 MHz, $CDCl_3$) δ 161.4, 158.2, 149.9, 149.2, 148.9, 137.3, 133.1, 130.3, 129.8, 129.6, 126.9, 121.7, 120.4, 114.8, 111.1, 109.2, 55.9, 55.9, 51.0, 46.8, 38.3, 12.0. HRMS (ESI) *m/z* calcd for $C_{24}H_{30}ClN_4O_2$ $[M+H]^+$ 441.2052, found 441.2052.

(E)-6-Chloro-2-(3,4-dimethoxystyryl)-4-(2-diisopropylaminoethyl)aminoquinazo--line (**9bc**). Yellow solid, yield 28%, m.p. 182~185 °C. ^1H NMR (400 MHz, $CDCl_3$) δ 7.96 (d, *J* = 15.7 Hz, 1H), 7.72 (d, *J* = 9.2 Hz, 1H), 7.63~7.58 (m, 2H), 7.22 (d, *J* = 1.8 Hz, 1H), 7.16 (dd, *J* = 8.3, 1.8 Hz, 1H), 7.07 (d, *J* = 15.7 Hz, 1H), 6.88 (d, *J* = 8.3 Hz, 1H), 6.70 (s, 1H), 3.94 (s, 3H), 3.91 (s, 3H), 3.74~3.66 (m, 2H), 3.19~3.12 (m, 2H), 2.89~2.83 (m, 2H), 1.12 (d, *J* = 6.5 Hz, 12H). ^{13}C NMR (100 MHz, $CDCl_3$) δ 161.5, 158.1, 149.9, 149.2, 148.8, 137.3, 133.1, 130.4, 129.8, 129.6, 126.9, 121.7, 120.3, 114.8, 111.1, 109.2, 56.0, 55.9, 47.8, 39.0, 30.9, 20.9. HRMS (ESI) *m/z* calcd for $C_{26}H_{34}ClN_4O_2$ $[M+H]^+$ 469.2365, found 469.2364.

(E)-6-Chloro-2-(3,4-dimethoxystyryl)-4-(1-piperidinylethyl)aminoquinazoline (**9bd**). Yellow solid, yield 64%, m.p. 85~87 °C. ^{1}H NMR (400 MHz, $CDCl_3$) δ 7.95 (d, J = 15.7 Hz, 1H), 7.74~7.70 (m, 2H), 7.63~7.59 (m, 1H), 7.22 (d, J = 1.8 Hz, 1H), 7.16 (dd, J = 8.3, 1.8 Hz, 1H), 7.06 (d, J = 15.7 Hz, 1H), 6.87 (d, J = 8.3 Hz, 1H), 6.75 (s, 1H), 3.93 (s, 3H), 3.91 (s, 3H), 3.83~3.78 (m, 2H), 2.72 (t, J = 5.9 Hz, 2H), 2.57~2.50 (m, 4H), 1.70~1.63 (m, 4H), 1.55~1.48 (m, 2H). ^{13}C NMR (100 MHz, $CDCl_3$) δ 161.3, 158.2, 149.9, 149.2, 148.8, 137.3, 133.1, 130.3, 129.7, 129.6, 126.9, 121.7, 120.8, 114.8, 111.1, 109.2, 56.8, 55.9, 55.9, 54.3, 37.4, 26.0, 24.3. HRMS (ESI) *m/z* calcd for $C_{25}H_{30}ClN_4O_2$ $[M+H]^+$ 453.2052, found 453.2050.

(E)-6-Chloro-2-(3,4-dimethoxystyryl)-4-[2-(morpholinyl)ethyl]-aminoquinazoline (**9be**). Yellow solid, yield 52%, m.p. 159~161 °C. ^{1}H NMR (400 MHz, $CDCl_3$) δ 7.94 (d, J = 15.7 Hz, 1H), 7.74 (d, J = 8.8 Hz, 1H), 7.67~7.60 (m, 2H), 7.21 (d, J = 1.8 Hz, 1H), 7.15 (dd, J = 8.3, 1.8 Hz, 1H), 7.06 (d, J = 15.7 Hz, 1H), 6.87 (d, J = 8.3 Hz, 1H), 6.43 (s, 1H), 3.93 (s, 3H), 3.91 (s, 3H), 3.85~3.77 (m, 6H), 2.76 (t, J = 6.0 Hz, 2H), 2.61~2.56 (m, 4H). ^{13}C NMR (100 MHz, $CDCl_3$) δ 161.3, 158.1, 150.0, 149.2, 148.8, 137.5, 133.3, 130.4, 129.8, 129.5, 126.7, 121.7, 120.4, 114.6, 111.1, 109.1, 67.0, 56.7, 55.9, 55.8, 53.4, 37.1. HRMS (ESI) *m/z* calcd for $C_{24}H_{28}ClN_4O_3$ $[M+H]^+$ 455.1844, found 455.1849 (the resonance of O–H was not observed in $CDCl_3$).

(E)-6-Chloro-2-(3,4-dimethoxystyryl)-4-(3-dimethylaminopropyl)aminoquinazoline (**9bf**). Yellow solid, yield 53%, m.p. 76~78 °C. ^{1}H NMR (400 MHz, $CDCl_3$) δ 8.88 (s, 1H), 7.93 (d, J = 15.7 Hz, 1H), 7.69 (d, J = 8.8 Hz, 1H), 7.62~7.57 (m, 2H), 7.22 (d, J = 1.8 Hz, 1H), 7.15 (dd, J = 8.3, 1.8 Hz, 1H), 7.06 (d, J = 15.7 Hz, 1H), 6.87 (d, J = 8.3 Hz, 1H), 3.93 (s, 3H), 3.91 (s, 3H), 3.87~3.82 (m, 2H), 2.70~2.66 (m, 2H), 2.44 (s, 6H), 1.97~1.91 (m, 2H). ^{13}C NMR (100 MHz, $CDCl_3$) δ 161.5, 158.6, 149.8, 149.1, 148.7, 137.1, 132.8, 130.2, 129.7, 129.5, 127.1, 121.7, 121.2, 115.2, 111.1, 109.2, 59.4, 55.9, 55.9, 45.2, 42.1, 24.3. HRMS (ESI) *m/z* calcd for $C_{23}H_{28}ClN_4O_2$ $[M+H]^+$ 427.1895, found 427.1896.

(E)-6-Chloro-2-(3,4-dimethoxystyryl)-4-(3-diethylaminopropyl)aminoquinazoline (**9bg**). Yellow solid, yield 24%, m.p. 78~80 °C. ^{1}H NMR (500 MHz, $CDCl_3$) δ 9.03 (s, 1H), 7.85 (d, J = 15.7 Hz, 1H), 7.61~7.56 (m, 2H), 7.48~7.43 (m, 1H), 7.13~7.10 (m,

1H), 7.07~7.03 (m, 1H), 6.97 (d, *J* = 15.7 Hz, 1H), 6.76~6.71 (m, 1H), 3.82 (s, 3H), 3.78 (s, 3H), 3.72~3.67 (m, 2H), 2.59~2.50 (m, 6H), 1.78~1.72 (m, 2H), 1.04~0.99 (m, 6H). ^{13}C NMR (100 MHz, $CDCl_3$) δ 161.4, 158.3, 149.7, 149.0, 148.5, 137.0, 132.5, 129.8, 129.8, 129.2, 126.9, 121.5, 121.2, 115.0, 111.0, 109.1, 55.7, 53.6, 46.7, 42.7, 29.6, 24.0, 11.2. HRMS (ESI) *m/z* calcd for $C_{25}H_{32}ClN_4O_2$ $[M+H]^+$ 455.2208, found 455.2206.

(E)-6-Chloro-2-(3,4-dimethoxystyryl)-4-(4-aminobutyl)aminoquinazoline (**9bh**). Yellow solid, yield 45%, m.p. 174~176 °C. ^{1}H NMR (400 MHz, CD_3OD) δ 8.11 (d, *J* = 2.2 Hz, 1H), 7.88 (d, *J* = 15.7 Hz, 1H), 7.66 (dd, *J* = 8.9, 2.2 Hz, 1H), 7.60 (d, *J* = 8.9 Hz, 1H), 7.21 (d, *J* = 1.8 Hz, 1H), 7.14 (dd, *J* = 8.3, 1.8 Hz, 1H), 6.96~6.89 (m, 2H), 3.89 (s, 3H), 3.85 (s, 3H), 3.80~3.76 (m, 2H), 2.97~2.92 (m, 2H), 1.89~1.82 (m, 2H), 1.81~1.73 (m, 2H). ^{13}C NMR (100 MHz, CD_3OD) δ 161.3, 158.8, 150.3, 149.3, 147.9, 138.0, 132.9, 130.3, 129.3, 127.9, 125.0, 121.5, 114.7, 111.4, 109.7, 55.1, 55.0, 39.9, 39.6, 29.4, 25.8. HRMS (ESI) *m/z* calcd for $C_{22}H_{26}ClN_4O_2$ $[M+H]^+$ 413.1739, found 413.1740 (the resonance of O-H and H-N-H were not observed in CD_3OD).

(E)-6-Chloro-2-(4-nitrostyryl)-4-(2-dimethylaminoethyl)aminoquinazoline (**10ba**). Yellow solid, yield 53%, m.p. 238~239 °C. ^{1}H NMR (400 MHz, $CDCl_3$) δ 8.25~8.22 (m, 2H), 8.01 (d, *J* = 15.9 Hz, 1H), 7.77~7.72 (m, 4H), 7.65 (dd, *J* = 8.8, 2.2 Hz, 1H), 7.30 (d, *J* = 15.9 Hz, 1H), 6.60 (s, 1H), 3.81~3.76 (m, 2H), 2.71~2.67 (m, 2H), 2.36 (s, 6H). ^{13}C NMR (100 MHz, $CDCl_3$) δ 160.1, 158.4, 148.6, 147.5, 143.0, 134.5, 133.4, 131.2, 130.0, 127.9, 124.1, 120.7, 114.9, 57.4, 45.2, 38.3. HRMS (ESI) *m/z* calcd for $C_{20}H_{21}ClN_5O_2$ $[M+H]^+$ 398.1378, found 398.1377.

(E)-6-Chloro-2-(4-nitrostyryl)-4-(2-diethylaminoethyl)aminoquinazoline (**10bb**). Yellow solid, yield 39%, m.p. 169~170 °C. ^{1}H NMR (400 MHz, $CDCl_3$) δ 8.24 (d, *J* = 8.7 Hz, 2H), 8.00 (d, *J* = 15.8 Hz, 1H), 7.77~7.72 (m, 4H), 7.65 (dd, *J* = 8.8, 1.8 Hz, 1H), 7.30 (d, *J* = 15.8 Hz, 1H), 6.97 (s, 1H), 3.82~3.76 (m, 2H), 2.88~2.84 (m, 2H), 2.70 (q, *J* = 7.1 Hz, 4H), 1.13 (t, *J* = 7.1 Hz, 6H). ^{13}C NMR (100 MHz, $CDCl_3$) δ 160.1, 158.4, 148.6, 147.5, 143.0, 134.5, 133.4, 131.3, 130.0, 127.9, 124.1, 120.7, 115.0, 51.1, 46.8, 38.2, 11.6. HRMS (ESI) *m/z* calcd for $C_{22}H_{25}ClN_5O_2$ $[M+H]^+$ 426.1691, found 426.1690.

(E)-6-Chloro-2-(4-nitrostyryl)-4-(2-diisopropylaminoethyl)aminoquinazoline (**10bc**). Yellow solid, yield 67%, m.p. 250~251 °C. ^{1}H NMR (400 MHz, $CDCl_3$) δ 8.24 (d, J = 8.7 Hz, 2H), 8.01 (d, J = 15.8 Hz, 1H), 7.78~7.63 (m, 5H), 7.31 (d, J = 15.8 Hz, 1H), 6.97 (s, 1H), 3.80~3.65 (m, 2H), 3.26~3.14 (m, 2H), 2.94~2.86 (m, 2H), 1.14 (d, J = 6.0 Hz, 12H). ^{13}C NMR (100 MHz, $CDCl_3$) δ 160.2, 158.3, 148.6, 147.5, 143.0, 134.5, 133.5, 133.4, 131.3, 130.0, 127.9, 124.1, 120.6, 115.1, 42.8, 38.9, 29.7, 20.7. HRMS (ESI) *m/z* calcd for $C_{24}H_{29}ClN_5O_2$ $[M+H]^+$ 454.2004, found 454.2033.

(E)-6-Chloro-2-(4-nitrostyryl)-4-(1-piperidinylethyl)aminoquinazoline (**10bd**). Yellow solid, yield 76%, m.p. 199~200 °C. ^{1}H NMR (400 MHz, $CDCl_3$) δ 8.23 (d, J = 8.8 Hz, 2H), 7.99 (d, J = 15.9 Hz, 1H), 7.78 (d, J = 2.2 Hz, 1H), 7.76~7.71 (m, 3H), 7.64 (dd, J = 8.9, 2.2 Hz, 1H), 7.29 (d, J = 15.9 Hz, 1H), 6.98 (s, 1H), 3.84~3.79 (m, 2H), 2.77~2.73 (m, 2H), 2.60~2.50 (m, 4H), 1.71~1.65 (m, 4H), 1.55~1.50 (m, 2H). ^{13}C NMR (100 MHz, $CDCl_3$) δ 160.1, 158.4, 148.6, 147.4, 143.0, 134.5, 133.4, 133.3, 131.3, 129.9, 127.9, 124.1, 120.9, 115.0, 56.8, 54.3, 37.4, 25.9, 24.2. HRMS (ESI) *m/z* calcd for $C_{23}H_{25}ClN_5O_2$ $[M+H]^+$ 438.1691, found 438.1691.

(E)-6-Chloro-2-(4-nitrostyryl)-4-[2-(morpholinyl)ethyl]aminoquinazoline (**10be**). Yellow solid, yield 70%, m.p. 221~223 °C. ^{1}H NMR (400 MHz, DMSO-d_6) δ 8.31 (d, J = 2.1 Hz, 1H), 8.19 (d, J = 8.7 Hz, 2H), 7.92~7.87 (m, 3H), 7.73 (dd, J = 8.9, 2.1 Hz, 1H), 7.67 (d, J = 8.9 Hz, 1H), 7.28 (d, J = 16.0 Hz, 1H), 3.78~3.72 (m, 2H), 3.60~3.57 (m, 4H), 2.64 (t, J = 6.8 Hz, 2H), 2.53~2.49 (m, 4H). ^{13}C NMR (100 MHz, DMSO-d_6) δ 160.2, 158.9, 148.9, 147.4, 143.1, 134.4, 134.0, 133.40, 130.1, 130.0, 128.8, 124.4, 122.6, 115.3, 66.7, 57.3, 55.4, 54.0, 38.3. HRMS (ESI) *m/z* calcd for $C_{22}H_{23}ClN_5O_3$ $[M+H]^+$ 440.1484, found 440.1487 (the resonance of O−H was not observed in DMSO-d_6).

(E)-6-Chloro-2-(4-nitrostyryl)-4-(3-dimethylaminopropyl)aminoquinazoline (**10bf**). Yellow solid, yield 42%, m.p. 244~246 °C. ^{1}H NMR (400 MHz, DMSO-d_6) δ 8.59 (t, J = 5.4 Hz, 1H), 8.43 (d, J = 2.2 Hz, 1H), 8.23 (d, J = 8.8 Hz, 2H), 8.04~7.98 (m, 3H), 7.78 (dd, J = 8.9, 2.2 Hz, 1H), 7.71 (d, J = 8.9 Hz, 1H), 7.33 (d, J = 15.9 Hz, 1H), 3.76~3.71 (m, 2H), 3.17~3.10 (m, 2H), 2.73 (s, 6H), 2.13~2.05 (m, 2H). ^{13}C NMR (100 MHz, $CDCl_3$ + CD_3OD) δ 163.8, 163.0, 151.7, 151.5, 146.7, 139.1, 137.7,

136.1, 135.6, 132.6, 132.0, 128.0, 125.9, 119.0, 59.8, 46.8, 41.7, 28.0. HRMS (ESI) *m/z* calcd for $C_{21}H_{23}ClN_5O_2$ $[M+H]^+$ 412.1535, found 412.1536.

(E)-6-Chloro-2-(4-nitrostyryl)-4-(3-diethylaminopropyl)aminoquinazoline (**10bg**). Yellow solid, yield 41%, m.p. 161~162 °C. ^{1}H NMR (400 MHz, $CDCl_3$) δ 9.38 (s, 1H), 8.23 (d, J = 8.1 Hz, 2H), 8.01 (d, J = 15.8 Hz, 1H), 7.76 ~ 7.69 (m, 4H), 7.64~7.60 (m, 1H), 7.30 (d, J = 15.8, 1H), 3.86~3.81 (m, 2H), 2.79~2.75 (m, 2H), 2.71 (q, J = 7.1 Hz, 4H), 1.95~1.88 (m, 2H), 1.17 (t, J = 7.1 Hz, 6H). ^{13}C NMR (100 MHz, $CDCl_3$) δ 160.5, 158.6, 148.5, 147.4, 143.2, 134.3, 133.7, 133.0, 130.9, 129.8, 127.9, 124.1, 121.3, 115.3, 54.2, 47.0, 43.3, 24.0, 11.4. HRMS (ESI) *m/z* calcd for $C_{23}H_{27}ClN_5O_2$ $[M+H]^+$ 440.1848, found 440.1847.

(E)-6-Chloro-2-(4-nitrostyryl)-4-(4-aminobutyl)aminoquinazoline (**10bh**). Yellow solid, yield 40%, m.p. 217~219 °C. ^{1}HNMR (400 MHz, DMSO-d_6) δ 8.41 (s, 2H), 8.19 (d, J = 8.5 Hz, 2H), 7.99~7.87 (m, 3H), 7.64~7.75 (m, 2H), 7.29 (d, J = 15.9 Hz, 1H), 3.67~3.60 (m, 2H), 2.74~2.68 (m, 2H), 1.78~1.70 (m, 2H), 1.60~1.52 (m, 2H). ^{13}CNMR (100 MHz, DMSO-d_6) δ 160.3, 159.0, 148.9, 147.4, 143.2, 134.5, 134.1, 133.4, 130.1, 130.0, 128.9, 124.4, 122.7, 115.4, 41.1, 40.8, 29.4, 26.3. HRMS (ESI) *m/z* calcd for $C_{20}H_{21}ClN_5O_2$ $[M+H]^+$ 398.1378, found 398.1381.

(E)-6-Chloro-2-(3,4-methylenedioxystyryl)-4-(2-dimethylaminoethyl)aminoquina--zoline (**11ba**). Yellow solid, yield 64%, m.p. 153~154 °C. ^{1}H NMR (400 MHz, DMSO-d_6) δ 8.33 (d, J = 2.2 Hz, 1H), 8.21 (t, J = 5.4 Hz, 1H), 7.83 (d, J = 15.8 Hz, 1H), 7.71 (dd, J = 8.9, 2.2 Hz, 1H), 7.64 (d, J = 8.9 Hz, 1H), 7.35 (d, J = 1.5 Hz, 1H), 7.09 (dd, J = 8.0, 1.5 Hz, 1H), 6.98 (d, J = 15.8, 1H), 6.93 (d, J = 8.0, 1H), 6.06 (s, 2H), 3.72 (q, J = 6.8, 2H), 2.56 (t, J = 6.8 Hz, 2H), 2.24 (s, 6H). ^{13}C NMR (100 MHz, DMSO-d_6) δ 161.1, 158.8, 149.1, 148.5, 136.9, 133.3, 130.9, 129.9, 129.4, 127.6, 123.7, 122.6, 115.1, 109.0, 106.5, 101.8, 58.1, 45.8. HRMS (ESI) *m/z* calcd for $C_{21}H_{22}ClN_4O_2$ $[M+H]^+$ 397.1426, found 397.1426.

(E)-6-Chloro-2-(3,4-methylenedioxystyryl)-4-(2-diethylaminoethyl)aminoquina--zoline (**11bb**). Yellow solid, yield 69%, m.p. 114~115 °C. ^{1}H NMR (400 MHz, $CDCl_3$) δ 7.92 (d, J = 15.7 Hz, 1H), 7.72 (d, J = 8.7 Hz, 1H), 7.64~7.59 (m, 2H), 7.17~7.15 (s, 1H), 7.07 (d, J = 8.0 Hz, 1H), 7.01 (dd, J = 15.7, 1H), 6.81 (d, J = 8.0

Hz, 1H), 6.65 (s, 1H), 5.99 (s, 2H), 3.75 (d, *J* = 5.0 Hz, 2H), 2.82~2.79 (m, 2H), 2.69~2.63 (m, 4H), 1.12~1.09 (m, 6H). ^{13}C NMR (100 MHz, $CDCl_3$) *δ* 161.3, 158.2, 148.9, 148.3, 148.2, 137.1, 133.1, 131.1, 130.4, 129.8, 127.1, 123.1, 120.4, 114.7, 108.5, 106.4, 101.3, 51.0, 46.8, 38.2, 12.0. HRMS (ESI) *m/z* calcd for $C_{23}H_{26}ClN_4O_2$ $[M+H]^+$ 425.1739, found 425.1738.

(E)-6-Chloro-2-(3,4-methylenedioxystyryl)-4-(2-diisopropylaminoethyl)aminoquina--zoline (**11bc**). Yellow solid, yield 82%, m.p. 175~176 °C. ^{1}H NMR (400 MHz, $CDCl_3$) *δ* 7.93 (d, *J* = 15.7 Hz, 1H), 7.72 (d, *J* = 9.2 Hz, 1H), 7.63~7.58 (m, 2H), 7.17 (d, *J* = 1.5 Hz, 1H), 7.08 (dd, *J* = 8.0, 1.5 Hz, 1H), 7.02 (d, *J* = 15.7 Hz, 1H), 6.82 (d, *J* = 8.0 Hz, 1H), 6.69 (s, 1H), 5.99 (s, 2H), 3.72~3.65 (m, 2H), 3.20~3.12 (m, 2H), 2.89~2.83 (s, 2H), 1.12 (d, *J* = 6.5 Hz, 12H). ^{13}C NMR (100 MHz, $CDCl_3$) *δ* 161.4, 158.1, 148.8, 148.3, 148.2, 137.1, 133.1, 131.1, 130.4, 129.8, 127.1, 123.1, 120.3, 114.8, 108.5, 106.4, 101.3, 47.8, 42.6, 38.9, 20.9. HRMS (ESI) *m/z* calcd for $C_{25}H_{30}ClN_4O_2$ $[M+H]^+$ 453.2052, found 453.2049.

(E)-6-Chloro-2-(3,4-methylenedioxystyryl)-4-(1-piperidinylethyl)aminoquinazoline (**11bd**). Yellow solid, yield 51%, m.p. 105~107 °C. ^{1}H NMR (400 MHz, $CDCl_3$) *δ* 7.91 (d, *J* = 15.7 Hz, 1H), 7.74~7.70 (m, 2H), 7.63~7.58 (m, 1H), 7.16 (s, 1H), 7.07 (d, *J* = 8.0 Hz, 1H), 7.01 (d, *J* = 15.7 Hz, 1H), 6.81 (d, *J* = 8.0 Hz, 2H), 5.99 (s, 2H), 3.82~3.76 (m, 2H), 2.71 (t, *J* = 5.5 Hz, 2H), 2.58~2.49 (m, 4H), 1.70~1.63 (m, 4H), 1.55~1.48 (m, 2H). ^{13}C NMR (100 MHz, $CDCl_3$) *δ* 161.2, 158.2, 148.8, 148.3, 148.2, 137.1, 133.1, 131.1, 130.4, 129.7, 127.1, 123.1, 120.7, 114.8, 108.4, 106.4, 101.3, 56.8, 54.3, 37.4, 26.0, 24.3. HRMS (ESI) *m/z* calcd for $C_{24}H_{26}ClN_4O_2$ $[M+H]^+$ 437.1739, found 437.1738.

(E)-6-Chloro-2-(3,4-methylenedioxystyryl)-4-[2-(morpholinyl)ethyl]aminoquina--zoline (**11be**). Gray solid, yield 45%. m.p. 109~111 °C. ^{1}H NMR (400 MHz, $CDCl_3$) *δ* 7.91 (d, *J* = 15.7 Hz, 1H), 7.74 (d, *J* = 8.8 Hz, 1H), 7.66~7.60 (m, 2H), 7.16 (d, *J* = 1.5 Hz, 1H), 7.07 (dd, *J* = 8.1, 1.5 Hz, 1H), 7.01 (d, *J* = 15.7 Hz, 1H), 6.81 (d, *J* = 8.0 Hz, 1H), 6.43 (s, 1H), 5.99 (s, 2H), 3.87~3.75 (m, 6H), 2.76 (t, *J* = 5.9 Hz, 2H), 2.61~2.56 (m, 4H). ^{13}C NMR (100 MHz, $CDCl_3$) *δ* 161.2, 158.1, 148.8, 148.4, 148.2, 137.3, 133.2, 131.0, 130.5, 129.9, 126.9, 123.2, 120.4, 114.6, 108.5, 106.4, 101.3,

67.0, 56.7, 53.4, 37.1. HRMS (ESI) *m/z* calcd for $C_{21}H_{22}ClN_4O_2$ $[M+H]^+$ 439.1531, found 439.1536.

(E)-6-Chloro-2-(3,4-methylenedioxystyryl)-4-(3-dimethylaminopropyl)aminoquina--zoline (**11bf**). Yellow solid, yield 57%, m.p. 150~152 °C. ^{1}H NMR (400 MHz, $CDCl_3$) δ 8.90 (s, 1H), 7.91 (d, J = 15.8 Hz, 1H), 7.71~7.68 (m, 1H), 7.60~7.56 (m, 2H), 7.16 (d, J = 1.5 Hz, 1H), 7.07 (dd, J = 8.0, 1.5 Hz, 1H), 7.00 (d, J = 15.8 Hz, 1H), 6.81 (d, J = 8.0 Hz, 1H), 5.98 (s, 2H), 3.86~3.81 (m, 2H), 2.68 (t, J = 5.5 Hz, 2H), 2.44 (s, 6H), 1.96~1.89 (m, 2H). ^{13}C NMR (100 MHz, $CDCl_3$) δ 161.4, 158.6, 148.7, 148.2, 148.2, 136.9, 132.8, 131.2, 130.2, 129.5 127.3, 123.1, 121.2, 115.2, 108.4, 106.4, 101.2, 59.5, 45.2, 42.2, 24.3. HRMS (ESI) *m/z* calcd for $C_{22}H_{24}ClN_4O_2$ $[M+H]^+$ 411.1582, found 411.1585.

(E)-6-Chloro-2-(3,4-methylenedioxystyryl)-4-(3-diethylaminopropyl)aminoquina--zoline (**11bg**). Yellow solid, yield 47%, m.p. 132~134 °C. ^{1}H NMR (400 MHz, $CDCl_3$) δ 9.17 (s, 1H), 7.91 (d, J = 15.7 Hz, 1H), 7.69 (d, J = 8.9 Hz, 1H), 7.66 (d, J = 2.2 Hz, 1H), 7.57 (dd, J = 8.9, 2.2 Hz, 1H), 7.17 (d, J = 1.6 Hz, 1H), 7.07 (dd, J = 8.0, 1.6 Hz, 1H), 7.01 (d, J = 15.7 Hz, 1H), 6.81 (d, J = 8.0 Hz, 1H), 5.98 (s, 2H), 3.85~3.79 (m, 2H), 2.76~2.72 (m, 2H), 2.69 (q, J = 7.1 Hz, 4H), 1.92~1.85 (m, 2H), 1.15 (t, J = 7.1 Hz, 6H). ^{13}C NMR (100 MHz, $CDCl_3$) δ 161.5, 158.4, 148.7, 148.2, 148.1, 136.9, 132.7, 131.2, 130.0, 129.6, 127.4, 123.1, 121.3, 115.1, 108.4, 106.4, 101.2, 54.2, 47.0, 43.1, 24.1, 11.5. HRMS (ESI) *m/z* calcd for $C_{24}H_{28}ClN_4O_2$ $[M+H]^+$ 439.1895, found 439.1895.

(E)-6-Chloro-2-(3,4-methylenedioxystyryl)-4-(4-aminobutyl)aminoquinazoline (**11bh**). Yellow solid, yield 65%, m.p. 180~182 °C. ^{1}H NMR (400 MHz, CD_3OD) δ 8.05 (d, J = 2.2 Hz, 1H), 7.82 (d, J = 15.7 Hz, 1H), 7.61 (dd, J = 8.9, 2.2 Hz, 1H), 7.56 (d, J = 8.9 Hz, 1H), 7.10 (d, J = 1.5 Hz, 1H), 7.00 (dd, J = 8.0, 1.5 Hz, 1H), 6.83 (d, J = 15.7 Hz, 1H), 6.78 (d, J = 8.0 Hz, 1H), 5.96 (s, 2H), 3.70~3.66 (m, 2H), 2.75~2.68 (m, 2H), 1.82~1.73 (m, 2H), 1.64~1.55 (m, 2H). ^{13}C NMR (100 MHz, CD_3OD) δ 161.2, 158.7, 148.4, 148.4, 147.8, 137.8, 132.8, 130.6, 130.1, 127.8, 125.2, 123.0, 121.5, 114.7, 108.0, 105.6, 101.4, 41.0, 40.6, 30.0, 26.1. HRMS (ESI) *m/z* calcd for $C_{21}H_{22}ClN_4O_2$ $[M+H]^+$ 397.1426, found 397.1427.

4.3. Cell cytotoxicity assay

Human cancer cell lines T24 (bladder cancer cell), MGC-803 (gastric cancer cell), DU145 (prostate cancer cell), PC-3 (prostate cancer cell), A549 (lung cancer cell) and human normal liver cell line HL-7702 cell lines used in this study were all obtained from the Institute of Biochemistry and Cell Biology, China Academy of Sciences. They were maintained in DMEM medium (T24, MGC-803, A549 and HL-7702 cell lines), RPMI-1640 Medium (DU145 cell lines) and DMEM-F12 medium (PC-3 cell); all were supplemented with 10% heat-inactivated fetal bovine serum (FBS) in a humidified atmosphere of 5% CO_2 at 37 °C.

The cytotoxicity of target compounds **9**~**11**, CP-31398 and Epirubicin against human cancer cell lines and human normal liver cell line HL-7702 cell lines was assayed by the microculture tetrozolium (MTT) assay. Compounds **9**~**11**, CP-31398 and Epirubicin dissolved in the culture medium with 1% DMSO to give various concentrations (1.25, 2.5, 5, 10, 20 μM, respectively) were added to the wells. Control wells contained supplemented media with 1% DMSO. After incubation for 48 h, MTT was added and then further incubated for 4 h. Removed the supernatant from each well and dissolved the purple formazan crystals by adding DMSO in each well. The plates were swirled gently for 10 min to dissolve the precipitate, and quantified by measuring the optical density (OD) of the plates at a wavelength of 570 nm on plate reader (TECAN, infinite, M1000). Each concentration was repeated in five wells and the same experimental conditions were provided for all compounds and MTT analysis was repeated three times for each cell line.

4.4. Agarose gel electrophoresis assay

The pBR322 DNA was incubated with a range of concentrations of **10ah** (50, 100, 200 μM) in TAE buffer for 3 h. Then, the reaction was terminated by the addition of loading buffer. The samples were electrophoresed in a 1% agarose gel and

stained with ethidium bromide before detection. The images of the DNA gel were captured using a BIO–RAD imaging system under UV–Vis transilluminator.

4.5. Spectroscopic studies on DNA binding

The 2.0 mM ct-DNA stock solution was stored at 4 °C for no more than 5 days before use. Compound **10ah** was prepared as 10 mM DMSO stock solutions for DNA binding studies.

In UV–Vis absorption spectrometry: the ct-DNA stock solution was added into the working solutions with increasing concentrations, wherein the [DNA]/[**10ah**] ration ranging from 0 to 1 at every 0.1 interval. After each addition, the solution was allowed to incubate for 5 min before the absorption spectrum was recorded. The absorption spectra were recorded in the range of 295–360 nm.

Fluorescence emission spectra were recorded with slit width of 5 nm for E_x and 5 nm for E_m, respectively. The competitive binding research was performed with a mixed solution of the ethidium bromide (EB, 10 μM) and ct-DNA (20 μM) in Tris–HCl buffer (pH 7.4), while gradually adding the concentrations of **10ah** ranging from 10 μM to 100 μM. For every addition, the test sample was shaken and equilibrated for 5 min, and then the fluorescence emission spectra were recorded. All the spectroscopic experiments were performed at 25 °C. Compound **10ah** was added with increasing concentrations to give the [**10ah**]/[DNA] ratios ranging from 0.5: 1 to 5: 1.

4.6. Cell cycle assay

In the cell cycle assay, MGC-803 cells were incubated for 48 h with **10ah** (0, 0.125, 0.25, 0.5 μM) and CP-31398 (0, 1, 5, 10 μM), respectively. Untreated and treated cells were harvested, then washed with phosphate-buffered saline (PBS), fixed and permeabilized in ice-cold 75% ethanol at –20 °C overnight. The cells were incubated with RNase at 37 °C for 30 min after washed with ice-cold PBS, and finally stained with propidium iodide (PI) at room temperature for 10 min in the dark and

immediately analyzed by flow cytometry (Becton Dickinson). Finally, analysis was performed with the system software (Cell Quest; BD Biosciences).

4.7. Apoptosis assay

Cell apoptosis analysis was performed by Annexin V-FITC/PI apoptosis detection kit (Becton−Dickinson, USA). Cells were seeded at sterile six-well culture plates and treated with **10ah** for 24 h. After treating, cells were harvested in cold PBS and collected by centrifugation for 5 min at 1000 rpm. Cells were resuspended at a density of 1×10^6 cells/mL in 1× binding buffer, stained with Annexin V-FITC and PI for 30 min at room temperature in the dark, and immediately analyzed by flow cytometer equipped with a 488 nm argon laser (Becton Dickinson).

4.8. Hoechst 33258 staining

Cells grown in sterile six-well culture plates were treated with **10ah** for the indicated time. The culture medium containing the **10ah** was removed, and cells were fixed in 4% paraformaldehyde for 10 min. After washing twice with PBS, cells were stained with 0.5 mL of Hoechst 33258 (Beyotime) for 5 min and washed twice with PBS. Nuclear staining was observed with a BioTek Cytation fluorescence microscope.

4.9. Caspase-3/9 activities assay

The measurement of caspase-3/9 activity was performed by CaspGLOW™ Fluorescein Active Caspase-3 and Caspase-9 Staining Kits, respectively. MGC-803 cells were treated with 2.5 μM of **10ah** for 24 h. 1 μL of FITC-DEVD-FMK (for caspase-3) or FITC-LEHD-FMK (for caspase-9) was added and incubated for 1 h at 37 °C, 5% CO_2. The analysis was performed using flow cytometer equipped with a

488 nm argon laser. Results were represented as the percent change of the activity comparing to the control.

4.10. Reactive oxygen species (ROS) generation assay

MGC-803 cells were seeded into six-well plates, and treated with **10ah** at 0.5, 1.0, 2.5 μM for 24 h. The cells were harvested, washed with cold PBS, and incubated with DCFH-DA (Beyotime, Haimen, China) at 37 □ for 30 min in the dark, and then washed three times with PBS. Finally, flow cytometer was used for measuring intracellular ROS generation by detecting the fluorescence intensity.

4.11. Intracellular Ca^{2+} measurement assay

MGC-803 cells were seeded into six-well plates, and treated with **10ah** at 0.5, 1.0, 2.5 μM for 24 h. The cells were harvested, washed with cold PBS, and incubated with Fluo-3 AM at 37 □ for 30 min in the dark, and then washed three times with PBS. Finally, detection of intracellular Ca^{2+} was carried out by flow cytometer (Becton Dickinson).

4.12. Mitochondrial membrane potential assay

MGC-803 cells were seeded into six-well plates, and treated with **10ah** at 0.5, 1.0, 2.5 μM for 24 h. The cells were harvested, washed with cold PBS, and incubated with JC-1 at 37 □ for 30 min in the dark, and then washed three times with wash buffer. Finally, $\Delta\Psi m$ analysis was performed by flow cytometry (Becton Dickinson).

4.13. Western blotting assay

MGC-803 cells (2×10^6) were cultured on dish and incubated overnight before experiments. MGC-80 cells were treated with **10ah** (0.5,1.0, 2.5 μM), **CP-31398** (5.0 μM) for 24 h, respectively. Cells were harvested and lysed using the lysis. The cell

extracts were separated by polyacrylamide-SDS gels, transferred to PVDF membrane, and probed with primary antibodies as indicated. The membrane was incubated with antirabbit IgG (AP-linked) and detected by an ECL western blot system (Kodak, USA).

4.14. In vivo xenograft model assay

Pathogen-free male BALB/C nude mice aged 6 weeks (Changzhou Cavens Experimental Animal Co., Ltd., Changzhou, China) were used to establish the MGC-803 xenograft model. All animal experiments were performed in accordance with the NIH guidelines for the care and use of laboratory animals. The mice were raised under controlled environmental conditions (12 h light-dark cycle at 24 °C and 60−85% humidity). Solid tumors were introduced by subcutaneous injection of 5×10^6 MGC-803 cells into the flank region of the nude mice (n = 6/group). The tumor-bearing nude mice with tumors at about 80 mm^3 were randomly divided into the vehicle control group and treatment group (n = 6/group) and treated via intraperitoneal injection with vehicle (5% DMSO in saline, *v*/*v*) or with 10 or 20 $mg\cdot kg^{-1}$ of **10ah** (dissolved in 0.5 mL DMSO and diluted with 9.5 saline to form a solution of 1.0 mg/mL or 2.0 mg/mL, respectively) per 2 days. Epirubicin (dissolved in 0.5 mL DMSO and diluted with 9.5 mL saline to form a solution of 1.0 mg/mL) was used as a positive control (10 $mg\cdot kg^{-1}$, per 2 days). The tumor size and body weight of the mice were measured three times a week. The tumor size was determined by measuring the length (l) and width (w) and calculating the volume ($V = lw^2/2$). The tumor growth inhibition (TGI) were calculated as follows: $TGI = (1 - TW_t/TW_c) \times 100\%$, where TW_c and TW_t are the tumor weight in the absence and presence of test compound.

4.15. Statistical Analysis.

All data are shown as mean ± standard deviation (SD) using two-tailed Student *t*

tests and *p* less than 0.05 was considered as the threshold for significance.

Acknowledgments

We are grateful for the financial support from the National Natural Science Foundation of China (81960638, 21362007, 21462008), the Guangxi Natural Science Foundation (2017GXNSFDA198045), the Foundation of State Key Laboratory for Chemistry and Molecular Engineering of Medicinal Resources (Guangxi Normal University, CMEMR2018-A1), Innovation Project of Guangxi Graduate Education (YCBZ2018032 and YCSW2017062).

Appendix A. Supplementary data

Supplementary data related to this article can be found at https://doi.org/

References

[1] D. Zhou, M.Z. Springer, D. Xu, D. Liu, A. Hudmon, K.F. MacLeod, S.O. Meroueh, Small molecules inhibit STAT3 activation, autophagy, and cancer cell anchorage-independent growth, Bioorg. Med. Chem. 25 (2017) 2995–3005.

[2] J. Mularski, K. Malarz, M. Pacholczyk, R. Musiol, The p53 stabilizing agent CP-31398 and multi-kinase inhibitors. Designing, synthesizing and screening of styrylquinazoline series, Eur. J. Med. Chem. 163 (2019) 610–625.

[3] E. Forcellini, S. Boutin, C.-A. Lefebvre, E.E. Shayhidin, M.-C. Boulanger, G. Rheaume, X. Barbeau, P. Lague, P. Mathieu, J.-F. Paquin, Synthesis and biological evaluation of novel quinazoline-4-piperidine sulfamide derivatives as inhibitors of NPP1, Eur. J. Med. Chem. 147 (2018) 130–149.

[4] D. Xu, L. Li, D. Zhou, D. Liu, A. Hudmon, S.O. Meroueh, Structure-based target specific screening leads to small-molecule CaMKII inhibitors, ChemMedChem 12 (2017) 660–677.

[5] H.S. Sutherland, I.Y. Hwang, E.S. Marshall, B.S. Lindsay, W.A. Denny, C.

Gilchrist, W.R. Joseph, D. Greenhalgh, E. Richardson, P. Kestell, A. Ding, B.C. Baguley, Therapeutic reactivation of mutant p53 protein by quinazoline derivatives, Invest. New Drugs 30 (2012) 2035–2045.

[6] A. Mrozek-Wilczkiewicz, D.S. Kalinowski, R. Musiol, J. Finster, A. Szurko, K. Serafin, M. Knas, S.K. Kamalapuram, Z. Kovacevic, J. Jampilek, A. Ratuszna, J. Rzeszowska-Wolny, D.R. Richardson, J. Polanski, Investigating the anti-proliferative activity of styrylazanaphthalenes and azanaphthalenediones. Bioorg. Med. Chem. 18 (2010) 2664-2671.

[7] J. Jampilek, R. Musiol, J. Finster, M. Pesko, J. Carroll, K. Kralova, M. Vejsova, J. O'Mahony, A. Coffey, J. Dohnal, J. Polanski, Investigating biological activity spectrum for novel styrylquinazoline analogues. Molecules 14 (2009) 4246-4265.

[8] G.M. Nepomuceno, K.M. Chan, V. Huynh, K.S. Martin, J.T. Moore, T.E. O'Brien, L.A.E. Pollo, F.J. Sarabia, C. Tadeus, Z. Yao, D.E. Anderson, J.B. Ames, J.T. Shaw, Synthesis and Evaluation of Quinazolines as Inhibitors of the Bacterial Cell Division Protein FtsZ, ACS Med. Chem. Lett. 6 (2015) 308–312.

[9] D.E. Anderson, M.B. Kim, J.T. Moore, T.E. O'Brien, N.A. Sorto, C.I. Grove, L.L. Lackner, J.B. Ames, J.T. Shaw, Comparison of Small Molecule Inhibitors of the Bacterial Cell Division Protein FtsZ and Identification of a Reliable Cross-Species Inhibitor, ACS Chem. Biol. 7 (2012) 1918–1928.

[10] M. Okano, J. Mito, Y. Maruyama, H. Masuda, T. Niwa, S.-i. Nakagawa, Y. Nakamura, A. Matsuura, Discovery and structure-activity relationships of 4-aminoquinazoline derivatives, a novel class of opioid receptor like-1 (ORL1) antagonists, Bioorg. Med. Chem. 17 (2009) 119–132.

[11] G.P. Zhikhareva, E.A. Berlyand, S.S. Liberman, L.N. Yakhontov, Synthesis and study of the antiinflammatory effect of 4-amino-2-styrylquinazolines, Khim.-Farm. Zh. 11 (1977) 58–62.

[12] N.Y. Moskalenko, L.N. Yakhontov, G.P. Zhikhareva, G.N. Pershin, V.V. Peters, M.I. Evstratova, L.I. Mastafanova, S.A. Rabinovich, E.V. Maksakovskaya, I.M. Kulikovskaya, 4-Amino-2-styrylquinazolines – a new class of antiprotozoal drugs, Khim.-Farm. Zh. 20 (1986) 437–446.

[13] G.P. Zhikhareva, L.I. Mastafanova, N.S. Bogdanova, V.V. Peters, I.S. Nikolaeva, G.N. Pershin, L.N. Yakhontov, Synthesis and study of the antiviral activity of substituted 4-(δ-diethylamino-α-methylbutylamino)-2-styrylquinazolines, Khim.-Farm. Zh. 12 (1978) 44–48.

[14] X.-X. He, Y.-N. Zhang, J.-W. Yan, J.-J. Yan, Q. Wu, Y.-H. Song, CP-31398 inhibits the growth of p53-mutated liver cancer cells in vitro and in vivo, Tumor Biol. 37 (2016) 807–815.

[15] V. Madka, Y. Zhang, Q. Li, A. Mohammed, P. Sindhwani, S. Lightfoot, X.-R. Wu, L. Kopelovich, C.V. Rao, p53-stabilizing agent CP-31398 prevents growth and invasion of urothelial cancer of the bladder in transgenic UPII-SV40T mice, Neoplasia 15 (2013) 966–974.

[16] C.V. Rao, J.M.R. Patlolla, L. Qian, Y. Zhang, M. Brewer, A. Mohammed, D. Desai, S. Amin, S. Lightfoot, L. Kopelovich, Chemopreventive effects of the p53-modulating agents CP-31398 and Prima-1 in tobacco carcinogen-induced lung tumorigenesis in A/J mice, Neoplasia 15 (2013) 1018–1027.

[17] J. Xu, L. Timares, C. Heilpern, Z. Weng, C. Li, H. Xu, J.G. Pressey, C.A. Elmets, L. Kopelovich, M. Athar, Targeting Wild-Type and Mutant p53 with Small Molecule CP-31398 Blocks the Growth of Rhabdomyosarcoma by Inducing Reactive Oxygen Species-Dependent Apoptosis, Cancer Res. 70 (2010) 6566–6576.

[18] L. Liu, T.-T. Yu, C.-C. Ren, L. Yang, S.-H. Cui, X.-A. Zhang, CP-31398 inhibits the progression of cervical cancer through reversing the epithelial mesenchymal transition via the downregulation of PAX2s, J. Cell. Physiol. 234 (2019) 2929–2942.

[19] L. Liu, L. Yang, H. Chang, Y.-n. Chen, F. Zhang, S. Feng, J. Peng, C.-c. Ren, X.-a. Zhang, CP-31398 attenuates endometrial cancer cell invasion, metastasis and resistance to apoptosis by downregulating MDM2 expression, Int. J. Oncol. 54 (2019) 942–954.

[20] G.-H. Zhang, J.-M. Yuan, G. Qian, C.-X. Gu, K. Wei, D.-L. Mo, J.-K. Qin, Y. Peng, Z.-P. Zhou, C.-X. Pan, G.-F. Su, Phthalazino[1,2-*b*]quinazolinones as p53 Activators: Cell Cycle Arrest, Apoptotic Response and Bak-Bcl-xl Complex Reorganization in Bladder Cancer Cells, J. Med. Chem. 60 (2017) 6853–6866.

[21] G.-H. Zhang, W.-B. Xue, Y.-F. An, J.-M. Yuan, J.-K. Qin, C.-X. Pan, G.-F. Su, Distinct novel quinazolinone exhibits selective inhibition in MGC-803 cancer cells by dictating mutant p53 function, Eur. J. Med. Chem. 95 (2015) 377–387.

[22] A. Mrozek-Wilczkiewicz, E. Spaczynska, K. Malarz, W. Cieslik, M. Rams-Baron, V. KryAitof, R. Musiol, Design, synthesis and in vitro activity of anticancer

styrylquinolines. The p53 independent mechanism of action. PLoS One 10 (2015) e0142678/0142671–e0142678/0142614.

[23] A. Mrozek-Wilczkiewicz, M. Kuczak, K. Malarz, W. Cieslik, E. Spaczynska, R. Musiol, The synthesis and anticancer activity of 2-styrylquinoline derivatives. A p53 independent mechanism of action. Eur. J. Med. Chem. 177 (2019) 338–349.

[24] R. Palchaudhuri, P.J. Hergenrother, DNA as a target for anticancer compounds: methods to determine the mode of binding and the mechanism of action, Curr. Opin. Biotechnol. 18 (2007) 497–503.

[25] J. Portugal, Challenging transcription by DNA-binding antitumor drugs, Biochem. Pharmacol. 155 (2018) 336–345.

[26] F. Jafari, H. Baghayi, P. Lavaee, F. Hadizadeh, F. Soltani, H. Moallemzadeh, S. Mirzaei, S.M. Aboutorabzadeh, R. Ghodsi, Design, synthesis and biological evaluation of novel benzo- and tetrahydrobenzo-[*h*]quinoline derivatives as potential DNA-intercalating antitumor agents, Eur. J. Med. Chem. 164 (2019) 292–303.

[27] R. Zhang, X.-Q. Song, R.-P. Liu, Z.-Y. Ma, J.-Y. Xu, Fuplatin: An Efficient and Low-Toxic Dual-Prodrug, J. Med. Chem. 62 (2019) 4543–4554.

[28] Q.-Q. Liu, K. Lu, H.-M. Zhu, S.-L. Kong, J.-M. Yuan, G.-H. Zhang, N.-Y. Chen, C.-X. Gu, C.-X. Pan, D.-L. Mo, G.-F. Su, Identification of 3-(benzazol--2-yl)quinoxaline derivatives as potent anticancer compounds: privileged structure-based design, synthesis and bioactive evaluation *in vitro* and *in vivo*, Eur. J. Med. Chem. 165 (2019) 293–308.

[29] J.-M. Yuan, K. Wei, G.-H. Zhang, N.-Y. Chen, X.-W. Wei, C.-X. Pan, D.-L. Mo, G.-F. Su, Cryptolepine and aromathecin based mimics as potent G-quadruplex-binding, DNA-cleavage and anticancer agents: Design, synthesis and DNA targeting-induced apoptosis, Eur. J. Med. Chem. 169 (2019) 144–158.

[30] S. Yogosawa, K. Yoshida, Tumor suppressive role for kinases phosphorylating p53 in DNA damage-induced apoptosis, Cancer Sci. 109 (2018) 3376–3382.

[31] Y. Yang, S. Karakhanova, W. Hartwig, J.G. D'Haese, P.P. Philippov, J. Werner, A.V. Bazhin, Mitochondria and Mitochondrial ROS in Cancer: Novel Targets for Anticancer Therapy, J. Cell. Physiol. 231 (2016) 2570–2581.

[32] R.R.M.L. La, G. Roest, G. Bultynck, J.B. Parys, Intracellular Ca^{2+} signaling and Ca^{2+} microdomains in the control of cell survival, apoptosis and autophagy, Cell

Calcium 60 (2016) 74–87.

[33] J. Li, N. Kwon, Y. Jeong, S. Lee, G. Kim, J. Yoon, Aggregation-Induced Fluorescence Probe for Monitoring Membrane Potential Changes in Mitochondria, ACS Appl. Mater. Interfaces 10 (2018) 12150–12154.

[34] G. Kroemer, L. Galluzzi, C. Brenner, Mitochondrial membrane permeabilization in cell death, Physiol. Rev. 87 (2007) 99–163.

[35] M.T. Bogert, R.A. Gortner, Researches on Quinazolines. Twenty-second Paper. On 2-Methyl-3-amino-4-quinazolone and Certain of Its Derivatives. J. Am. Chem. Soc. 31 (1909) 943–947.

[36] A.J. Tomisek, B.E. Christensen, Quinazolines. VI. Syntheses of certain 2-methyl-4-substituted quinazolines. J. Am. Chem. Soc. 70 (1948) 2423–2425.

[37] I.M. Heilbron, F.N. Kitchen, E.B. Parkes, G.D. Sutton, Chemical reactivity and conjugation. II. The reactivity of the 2-methyl group in the 4-quinazoline series. J. Chem. Soc., Trans. 127 (1925) 2167–2175.

[38] M.T. Bogert, G.D. Beal, Researches on Quinazolines. XXIX. A Further Study of the Stilbazoles, Hydrazones and Schiff Bases of the 4-Quinazolone Group. J. Am. Chem. Soc. 34 (1912) 516–524.

[39] D. Papa, M.T. Bogert, Quinazolines. XLIII. Synthesis of a quinazoline derivative structurally analogous to cusparine. J. Am. Chem. Soc. 58 (1936) 1701–1703.

Highlights

(1) 48 2-styryl-4-aminoquinazoline as CP-31398 analog were synthesized.

(2) Compounds cleave double-strand DNA and activates p53 pathway.

(3) Induce cell cycle arrest and apoptosis at low concentration.

(4) Suppress tumor via a mechanism quite differ from CP-31398.

(5) Display potent antitumor efficiency *in vivo* with low toxicity.

Conflict of interest statement

We declare that we do not have any commercial or associative interest that represents a conflict of interest in connection with the work submitted.